Novel systems analysis elucidates the influence of personalized variation in microbiome composition on metronidazole efficacy in bacterial vaginosis

Christina Lee
University of Michigan
Ryan Cheu
University of Miami
Melissa Lemke
University of Michigan–Ann Arbor https://orcid.org/0000-0003-1860-4550
Andrew Gustin
University of Washington https://orcid.org/0000-0002-8760-8320
Michael France
University of Maryland, Baltimore
Benjamin Hampel
University of Zurich
Andrea Thurman
Eastern Virginia Medical School
Gustavo Doncel
Eastern Virginia Medical School
Jacques Ravel
University of Maryland, Baltimore https://orcid.org/0000-0002-0851-2233
Nichole Klatt
University of Miami
Kelly Arnold (kbarnold@umich.edu)
University of Michigan–Ann Arbor

Article

Keywords: systems analysis, bacterial vaginosis (BV), metronidazole efficacy

Posted Date: September 3rd, 2020

DOI: https://doi.org/10.21203/rs.3.rs-66397/v1

Version of Record: A version of this preprint was published at Nature Communications on December 1st, 2020. See the published version at https://doi.org/10.1038/s41467-020-19880-w.

Novel systems analysis elucidates the influence of personalized variation in microbiome composition on metronidazole efficacy in bacterial vaginosis

Christina Y. Lee[1*], Ryan K. Cheu[2,3*], Melissa M. Lemke[1], Andrew Gustin[2,3], Michael France[4], Benjamin Hampel[5], Andrea Thurman[6], Gustavo F. Doncel[6], Jacques Ravel[4], Nichole R. Klatt[2,3#], Kelly B. Arnold[1#]

[1]Department of Biomedical Engineering, University of Michigan, Ann Arbor, MI, United States of America

[2]University of Miami Department of Pediatrics, University of Miami, Miami, FL, United States of America

[3] Department of Pharmaceutics, University of Washington, Seattle, WA, United States of America

[4]Institute for Genome Sciences and Department of Microbiology and Immunology, University of Maryland School of Medicine, Baltimore, MD, 21201, United States of America

[5]Division of Infectious Diseases and Hospital Epidemiology, University of Zurich, 8901, Zürich, Switzerland

[6]Eastern Virginia Medical School, CONRAD, Norfolk, VA, United States of America

[*] These authors contributed equally to this work.

[#]co-senior authors

Address correspondence to: Kelly B. Arnold (kbarnold@umich.edu), Nicole R. Klatt (nklatt@med.miami.edu)

Abstract

Bacterial vaginosis (**BV**) is a syndrome of the female reproductive tract associated with adverse reproductive outcomes and characterized by a shift from a *Lactobacillus* (**LB**)-dominant vaginal microbiota to a polymicrobial, anaerobic microbiota, consistently colonized by strains of *Gardnerella vaginalis* (***Gv***). The first-line treatment for BV is metronidazole (**MNZ**); however, treatment failure and recurrence rates remain high. To gain insight into complex interactions between target species (*Gv*) and non-target *Lactobacillus* species (*Lactobacillus iners (**Li**))* with MNZ and understand their respective roles in efficacy, we developed an ordinary differential equation model that predicts bacterial growth as a function of drug uptake, metabolism, proliferation, and MNZ sensitivity. Model findings revealed a critical factor in MNZ efficacy may be *Li* sequestration of MNZ, and that efficacy decreases when the relative abundance of Li is higher pre-treatment. These results were validated in *Gv* and *Li* co-cultures ($p < 0.001$), and in two clinical cohorts, finding women with recurrent BV had significantly lower pre-treatment levels of BV-associated bacteria relative to *Lactobacillus spp.* ($p = 0.0366$; $p = 0.0484$). Overall, model results support a mechanism where non-target *Lactobacillus* species sequester MNZ from BV-associated target species, such as *Gv*, promoting BV recurrence by reducing MNZ bioavailability.

Main Text

Bacterial vaginosis (**BV**) is a condition that affects 30-60% of women worldwide,[1,2] with negative outcomes involving increased susceptibility to sexually transmitted infections (**STIs**), and adverse reproductive outcomes including pre-term birth.[3–7] BV is characterized by a shift from *Lactobacillus* species (spp.)-dominated vaginal microbiota to a wide array of anaerobic bacteria including *Gardnerella vaginalis* (***Gv***) and *Atopobium vaginae.*[8,9,10] Treatment of symptomatic BV with metronidazole (**MNZ**) is aimed to restore *Lactobacillus*-dominated microbiota, but because BV is not caused by a single pathogen easily targeted with antimicrobial therapy, recurrence rates are reported to be 57-90% within 12 months of receiving adequate treatment.[11,12,13,14] Recurrence is associated with several host factors including previous episodes of BV, douching, and sexual activity, but no one factor emerges as a single driver of treatment failure.[11,15–17,18] Additionally, associations between vaginal microbiota composition and BV recurrence have been reported but remain poorly understood, with several studies citing conflicting results.[15,17,19]

Recent improvements in 16S rRNA sequencing have enhanced the ability to identify and more accurately quantify the composition of the vaginal microbiota in BV,[20,21] finding that the transition is frequently associated with an abundance of *Lactobacillus iners* (***Li***).[22,23] Despite the association between *Li* and incidence of BV, identifying how *Li* dictates communities of optimal and non-optimal microbiota remains elusive, as the vaginal microbiota can change significantly over time and vary between women[24,25,26,], especially in the presence of MNZ. The recommended treatment regimen for BV consists of oral or vaginal MNZ oriented towards selectively targeting anaerobic bacteria with little

effect on *Lactobacillus* spp.,[27,28] but high variability in efficacy indicates that further study is required to understand the reestablishment of optimal vaginal microbiota ecosystems.

Recent research in the HIV microbicide field has highlighted the importance of vaginal microbiome composition in drug treatment efficacy. In a landmark study, variability in tenofovir (TFV) microbicide efficacy was accounted for by differences in the vaginal microbiome, specifically the presence of the non-target species *Gv,* which were shown to metabolize TFV.[29] Likewise for MNZ treatment of *Trichomonas vaginalis*, a proposed mechanism of treatment failure was decreased bioavailability of MNZ due to the absorbance of the antibiotic by other microorganisms in the vagina.[30,31,32] In the context of BV, it is possible that the mechanisms underlying MNZ treatment failure could be related to complex inter-species growth dynamics and absorption of MNZ. We propose that variability in MNZ efficacy may result from underlying differences in MNZ uptake and susceptibility in target and non-target species, and therefore would be highly dependent on individual differences in pre-treatment vaginal microbiota composition.

To test this hypothesis, we developed an ordinary differential equation (ODE) model that uses experimentally measured parameters (MNZ internalization by bacteria, metabolism and bacterial antibiotic susceptibility) to predict *Li* and Gv growth dynamics with MNZ treatment. Ultimately, this model revealed the surprising insight that a critical factor in MNZ efficacy may be *Li* sequestration of MNZ, and that efficacy is predicted to be significantly reduced in individuals with higher pre-treatment amounts of the non-target species *Li* relative to the target species *Gv.* We experimentally validated this finding with *in vitro* co-cultures, and used more complex computational frameworks to illustrate that this behavior would also be expected in microbial environments with additional species,

interspecies interactions and stain variability. Finally, we validated results in cervicovaginal samples from BV-infected women treated with MNZ in two different clinical cohorts.[33,34] We propose that quantitative evaluation of target bacteria and non-target *Lactobacillus* spp. interactions with MNZ will provide new insight into personalized differences in BV recurrence and treatment failure.

Results

Computational ODE model elucidates an important role for L. iners sequestration of MNZ from G. vaginalis

To determine how MNZ treatment efficacy can be altered by bacterial-mediated interactions *in vitro*, we created an ODE model to predict growth of *Gv* and *Li* upon co-culture and treatment with MNZ (Fig. 1a). Parameters for each bacterial species were obtained by least squares fitting of *in vitro* kinetic data and dose-response curves for MNZ exposure with each species in monoculture (fig. S1, S2, Table S1), before the ODE model was used to predict co-culture conditions with *Gv* and *Li* both interacting with extracellular MNZ. The model assumes that *Gv* and *Li* internalize or sequester MNZ at rates $k_{int\text{-}Gv}$ and $k_{int\text{-}Li}$, respectively, and *Gv* can convert MNZ to the stable metabolite, acetamide and unknown metabolites at rate k_{met}.[35] The model additionally assumes logistic growth at rates $k_{grow\text{-}Gv}$ and $k_{grow\text{-}Li}$, with carrying capacities of K_{Gv} and K_{Li} and growth inhibition by MNZ toxicity at rates $k_{kill\text{-}Gv}$ and $k_{kill\text{-}Li}$ in a dose-dependent manner based on 50% effective concentrations of MNZ on *Gv* and *Li* ($EC50_{Gv}$, $EC50_{Li}$).[36,37] Since MNZ is a pro-drug that is activated when internalized by anaerobic bacteria, the cytotoxicity of MNZ in the model

is dependent on the intracellular concentration of MNZ rather than extracellular MNZ concentration; however, we used the external MNZ concentration as the basis for EC50 of internalized MNZ, as experimentally determining the intracellular level of MNZ per cell was challenging and the main goal was to capture the relative sensitivity between *Gv* and *Li*.[27,28,30,38]

To identify model parameters that were most critical for decreasing *Gv* growth, we performed a 1-dimensional (1D) sensitivity analysis by altering each parameter three orders of magnitude above and below baseline and evaluated *Gv* growth (Fig. 1b & c). Growth was scaled relative to the predicted growth in an unperturbed co-culture based on the time point and initial population sizes evaluated and is referred to as percent maximum growth. The sensitivity analysis identified *Gv* growth as highly dependent on the MNZ internalization/sequestration rate into *Li* ($k_{int\text{-}Li}$). A 50-fold increase in this rate increased the growth of *Gv* from 7.42% to 69.5% its maximal growth upon 48h treatment with MNZ, where percent maximal growth describes the expected proportion of cell density with antibiotic treatment relative to cell density with the same initial culture conditions without antibiotic (Fig. 1c). Likewise, changing the MNZ internalization rate into *Gv* ($k_{int\text{-}Gv}$) has similar effects on *Li*, where increasing this rate 50-fold resulted in 89.7% *Li's* maximal growth (fig. S3a). Overall, these results illustrate how MNZ efficacy in inhibiting *Gv* growth is influenced by the competition between each bacterium to internalize the drug.

From this result we hypothesized that the relative quantity of cells internalizing MNZ (ratio of *Gv* and *Li*) could significantly influence growth of both strains. We tested this hypothesis in our computational framework by predicting *Gv* survival after varying the

starting ratio of *Gv* to *Li* (**Gv:Li ratio**) from 1,000x fold to 0.001x. Results indicated that altering the initial Gv:Li ratio influences the growth of both *Gv* and *Li*. Counterintuitively, *Gv* survival was high when *Li* initially outnumbers *Gv* 1,000x and *Li* growth is optimal when *Gv* initially exceeds *Li* 1,000x (Fig. 1d). Stated differently, the model suggested that more *Gv* present at MNZ treatment initiation resulted in a better treatment outcome. The importance of MNZ internalization rate into *Li* became more apparent as *Li* became the predominating species, leading to increased growth of *Gv* (Fig. 1e). This result additionally supports that *Li* competes with *Gv* to internalize or sequester extracellular MNZ, as when one bacterial strain is in excess, it likely depletes available extracellular MNZ and decreases the amount of drug internalized by the non-dominating bacterial strain.

We used our model to explore this ratio-dependent behavior over a range of relevant MNZ concentrations extending from 100 μg/ml to 1,600 μg/ml, as estimates for vaginal accumulation range from 20 μg/ml to greater than 1,000 μg/ml (Fig. 2a, b).[39,40] Doses below 100 μg/ml had no effect on *Gv* or *Li* growth and doses above 1,600 μg/ml exhibited near complete cell killing for both bacterial strains (Fig. 2a & b); these data are in agreement with experimentally determined effective concentrations of MNZ on *Gv* and *Li* cultured individually (fig. S2 c-d). However, for doses between 100 and 1,600 μg/ml there were significant differences dependent on the initial Gv:Li ratio, where MNZ was most efficacious in eliminating *Gv* when more *Gv* than *Li* was present.

Model validation in Gv / Li co-cultures

We validated these counterintuitive model predictions experimentally *in vitro* by varying the initial *Gv:Li* ratios in the presence of 500 μg/ml MNZ and tracking growth for 48h (Fig. 2c, d). Experimental measurements confirmed model predictions that MNZ efficacy for inhibiting *Gv* growth decreased when *Li* was initially dominant ($p < 0.0001$, $t = 6.985$, $df = 34$), and were not significantly different than model predictions (0.001x Gv:Li, $p = 0.4297$, $t = 0.8087$, $df = 17$; 1,000x Gv:Li ratio, $p = 0.6891$, $t = 0.4070$, $df = 17$Fig. 3c), with *Gv* exhibiting a predicted 30.3% and experimental 41.4% ± 13.3% maximal growth after treatment when *Li* was initially dominant compared to a predicted 2.1% and experimental 9.4% ± 13.8% maximal growth when *Gv* initially was dominant. *Li* growth in the presence of 500 μg/ml MNZ was also dependent on the initial Gv:Li ratio, where MNZ inhibited *Li* growth the most when *Li* was initially dominant, 7.2% ± 3.9% maximal growth compared to when *Gv* was initially dominant, 70.5% ± 33.8% ($p < 0.0001$, $t = 7.908$, $df = 34$, Fig. 2d). Notably, the model over-predicted the growth of the *Li* population when *Li* was initially dominant (0.001x Gv:Li), where the model prediction of 23.9% maximal growth was over 3-fold higher than experimentally observed, 7.19% ± 3.91% growth (0.001x Gv:Li experiment vs simulation, $p < 0.0001$, $t = 18.15$, $df = 17$), suggesting efficacy dependence on a high pre-treatment Gv:Li ratio may be even greater than that predicted by the model. Experimental and model predictions of *Li* growth were not significantly different when *Gv* was initially dominant (1,000x GV:LI, $p = 0.1970$, $t = 1.343$, $df = 17$). Likewise, model predictions of MNZ and MNZ metabolite concentrations were not significantly different from experimental results in cultures starting with a 0.001x Gv:Li ratio (extracellular MNZ: $p = 0.2545$, $t = 1.178$, $df = 17$, intracellular MNZ: $p = 0.3356$, $t =$

0.9910, df = 17 acetamide: p = 0.8341, t = 0.1567, df = 17), but predictions for extracellular MNZ, intracellular MNZ, and acetamide concentrations in cultures with a 1,000x Gv:Li ratio did vary significantly from experimental data (fig. S4). The deviation of model predictions when *Gv* is initially dominant suggests that experimental investigation of detailed mechanisms of *Gv* interactions with MNZ is warranted (for example the potential ability of *Gv* to externally degrade MNZ). Despite some deviation of peripheral model predictions from experimental measurements, the Gv:Li ratio-dependent trends were reproduced by the model. The dependency on initial culture ratios of *Gv* to *Li* on growth suggests that non-target bacteria that sequester MNZ could significantly alter drug efficacy.

We observed some variation in the sensitivity (EC50) of *Li* to MNZ. Variability in minimum inhibitory concentrations (MIC) estimations have been reported, as changes in culture conditions including incubation length and the inoculum effect can influence the apparent sensitivity of bacteria to antibiotic.[37,41] Additionally, the sensitivity of *Lactobacillus* sp. and *Gv* to MNZ and their MICs are reported to range from 500 µg/ml – 4,000 µg/ml and 0.75 µg/ml to greater than 256 µg/ml, respectively.[42–44] To ascertain whether our results would be influenced by variation in *Li* sensitivity to MNZ, we repeated the simulations over a range of EC50 values. To represent reported resistance of *Lactobacillus* sp. *in vitro,* we increased the EC50 value of *Li* to be 10-fold higher than *Gv* ($EC50_{Li}$ = 4,200 µg/ml). MNZ efficacy in inhibiting *Gv* growth was similarly decreased at low Gv:Li ratios (36.5% max growth at 0.001x Gv:Li) compared to high Gv:Li ratios (3.96% max growth at 1000x Gv:Li, fig. S5a). *Li* had little to no susceptibility over the range of MNZ concentrations tested (fig. S5b). Additionally, these EC50 values replicated trends

in experimental data for growth kinetics (fig. S2d & h versus S5c & d). These results support that the initial Gv:Li ratio dependent trends in MNZ efficacy for inhibiting *Gv* growth are independent of *Li's* sensitivity to MNZ.

The model identifies optimal MNZ doses that can shift a G. vaginalis dominant population to a L. iners dominant population in-vitro

We next used the model to determine specific combinations of MNZ concentrations and initial Gv:Li ratios that resulted in optimal final *Li* proportion after 48 MNZ exposure. The initial Gv:Li ratio was highly associated with the final Gv:Li ratio for doses of MNZ greater than 250 µg/ml (Fig. 3a). Interestingly, cultures that were initially *Li* dominant (0.001x *Gv*:*Li*), were nearly insensitive to any dose of MNZ, resulting consistently with >50% *Gv* (Fig. 3a). This result carries the surprising implication that women with *Li*-dominant vaginal microbiomes at treatment initiation are likely to undergo recurrence, regardless of MNZ dose. Of note, cultures that were originally *Gv* dominant (Gv:Li > 1) were the most likely to be *Li* dominated after 48h exposure to MNZ. Experimental data supported these trends, as the simulation predictions were not significantly different for the final proportion of *Li* at 500 µg/ml for 1,000x ($p = 0.6798$, $t = 0.4202$, $df = 17$). The model did over-estimate the final proportion of *Li* at the 0.001x Gv:Li ratio (predicting a 44.1% proportion of *Li* compared to 14.2% $\pm$ 7.16% obtained experimentally); however, this result suggests an even more significant reduction in *Li* proportion when *Gv* is initially dominant ($p = 0.008$, $t = 4.056$, $df = 17$).

A phase diagram of MNZ therapy outcomes at 48h was created to characterize both *Li* and *Gv* endpoint growth dynamics, which depict either an increase/expansion or decrease in population size relative to the initial population. The optimal growth dynamics

would depict the expansion of only the *Li* population and the least optimal growth dynamics would be the expansion of only *Gv.* A decrease in both populations is additionally not optimal, as lower levels of beneficial microbiota are often associated with opportunistic infections or overgrowth of non-optimal species.[45,46] We observed that higher initial Gv:Li ratios in conjunction with MNZ concentrations over 250 µg/mL were more likely to result in optimal final growth dynamics where the *Li* bacterial population was the only population expanding (Fig. 3b). Likewise, it was possible for only the *Gv* population to grow and the *Li* population to decrease when the initial Gv:Li ratio was less than 1x. Interestingly, the diagram predicts that it is possible that both *Gv* and *Li* populations would decrease for intermediate ratios of Gv:Li, which expand to include a wider range of ratios as the dose of MNZ is increased. Overall, *in vitro* co-culture experimental data supported the model predictions for endpoint growth dynamics, with 15 of 18 samples agreeing with the dynamics predicted by the phase diagram for the 1,000x Gv:Li, 500 µg/ml group and for all 18 samples agreeing with the predictions for the 0.001x Gv:Li ratio, 500 µg/ml group (Fig. 3b, right). This result reinforces the importance of pre-treatment Gv:Li ratio on post-treatment bacterial community composition.

The pre-treatment Gv:Li ratio and MNZ sequestration by Li is predicted to influence MNZ efficacy in microbial environments with interspecies interactions and strain variability

While our model results emphasize the importance of pre-treatment Gv:Li ratios in MNZ efficacy in co-cultures, BV in women is more complex, and involves interspecies interactions and strain variability across many different bacterial species. In order to

evaluate the above results in more complex settings that include multiple species, interspecies interactions, and strain variability, we created three additional model structures (Fig. 4a-d). In Model B and Model D, we account for potential interspecies interactions, such as amensalism between *Lactobacillus* spp. and BV-associated bacteria and commensal or mutualistic behavior within BV-associated bacteria subpopulations and *Lactobacillus* spp. (Fig. 4a & d).[47–51] In Models C and D we add additional representative species; a second BV-associated species and second *Lactobacillus* sp. (Fig. 4c & d). In order to address potential variability in associated parameters, we randomly selected parameter values from physiologically relevant ranges determined from previously published studies (Table S2 & S3). Notably, across all four model structures we found that higher initial relative amounts of BV-associated bacteria to *Lactobacillus* spp. had higher relative post-antibiotic levels of *Lactobacillus* spp. (BV:LB ratio, Fig. 4e-f, fig. S6, $P < 1E\text{-}6$, $P < 1E\text{-}6$, $P < 1E\text{-}6$, $P < 1E\text{-}6$). This result held for a range of ratios (0.6x BV:LB and 100x BV:LB) chosen to reflect the observed relative abundance of *Lactobacillus* spp. in BV positive women (60% - 1.0%).[52] Moreover, for each of these model structures, the global sensitivity analyses consistently selected the MNZ internalization/sequestration parameter (k_{int}) and the initial relative abundance of BV-associated bacteria to *Lactobacillus* sp. (BV:LB ratio) as significantly sensitive parameters in post-antibiotic treatment *Lactobacillus* spp. relative abundance. Variability in *Gv* sensitivity to MNZ (EC50) and growth rate were also selected as critical parameters in dictating response to MNZ treatment, which of interest as there is significant variability across *Gv* subclasses in terms of resistance to MNZ, and metabolism.[53] Furthermore, when models were modified such that *Lactobacillus* spp. could not internalize/sequester

MNZ, the ratio-dependent effect was abrogated, and was additionally independent of sensitivity of *Lactobacillus spp.* to MNZ (fig. S7a-b). Altogether, this provides additional quantitative evidence that *Lactobacillus* spp. sequestration of MNZ may contribute to BV recurrence in more complex microbial environments.

Decreased pre-treatment BV:LB ratio is associated with BV recurrence in clinical samples

We next evaluated whether the influence of initial BV:LB ratio on MNZ efficacy is observed clinically. We compared the pre-treatment ratio of BV-associated bacteria to *Lactobacillus* spp. (BV:LB ratio) in vaginal samples collected from women who underwent MNZ treatment for BV and were cured or experienced recurrence, in two clinical studies; the UMB-HMP study[33] (n = 11) and CONRAD BV study[34] (n = 33). We chose to evaluate each study separately to minimize effects of differences in sample collection and in methods of microbial species measurements. In the UMB-HMP cohort, 11 women were observed over the course of 10 weeks and provided cervicovaginal lavage (CVLs) samples each day for quantification of relative microbial abundances by sequencing of the V3 and V4 regions of 16S rRNA. Patients underwent treatment for BV that consisted of one week of 500-mg oral MNZ, taken twice daily. Of the 11 women, 8 met inclusion criteria and were classified as recurrent or cured dependent on Nugent scoring, where recurrent patients were described as women who responded to treatment but exhibited a second episode of BV during the 10-week period (Table S2). Results resonated with model predictions where individuals who experienced recurrence had higher amounts of *Lactobacillus* spp. relative to BV-associated bacteria (lower BV:LB ratios, $P = 0.0366$) and tended to have higher abundances of *Lactobacillus* spp., particularly *Li,* but abundance

of individual species were not statistically significant after adjustment for multiple comparisons (P = 0.109, Fig. 5a fig. S8a). Additionally, *Gv* relative abundance was not significantly different between groups (P = 0.984, fig. S8b). Furthermore, when we analyzed the specific species in the original two-species model, we also observed similar results where cured women had significantly higher ratios of *Gv* to *Li* (p = 0.0249, Fig. 6b). In is important to note that since the Gv:Li ratio comparison was a selective analysis, we did not correct for multiple comparisons based on individual species in the original data set (over ~190 species measured). These results support both the *in vitro* experimental data and model results that predicted a lower efficacy of MNZ treatment when a lower ratio of *Gv to Li* was present pre-treatment.

We also evaluated model findings in a second clinical cohort, the CONRAD BV study, which consisted of 33 women whose vaginal microbiome was sampled at enrollment in the study, one week after MNZ treatment and one month after MNZ treatment. Relative abundances were determined by sequencing of the V4 region of the 16S rRNA. Women were excluded from this subset analysis if they failed to finish antibiotic regimen, contracted a secondary vaginal infection, did not respond or had delayed response of treatment. Of the 33 women, 21 met inclusion criteria and were evaluated by molecular-BV criteria (dominance of *Lactobacillus* spp.) at one week and one month, with women exhibiting a vaginal microbiota composition of less than 50% *Lactobacillus* sp. classified as BV positive. The group analyzed consisted of women who were cured (n=10) and or were determined to have recurrent BV (n=11; *Lactobacillus* was dominant at one week, but molecular-BV returned after one month, Table S3). Similar to the previous study, we found that women who experienced recurrence had higher levels

of *Lactobacillus* spp. relative to BV-associated bacteria (lower BV:LB ratio, P = 0.0484, Fig. 5c). Comparison of CLR-transformed relative abundance did not result in statistically significant differences for *Li* or *Gv,* but tended to support the trend of recurrent women having higher *Li* and lower *Gv* (fig. S8 c & d, P = 0.526, P = 0.539). Similarly, analysis of the Gv:Li ratio supported higher pre-treatment Gv relative to Li was associated with better treatment outcomes (Fig. 5d; p = 0.0191). Though preliminary and limited by low sample numbers, these results support the model predictions and suggest that successful BV treatment could be driven by competition for MNZ, where non-target bacterial populations, *Lactobacillus* spp., like *Li* sequester MNZ away from target bacterial populations like *Gv*, *A. vaginae, Sneathia,* etc., ultimately decreasing MNZ efficacy.

Discussion

Here we show a new, highly personalized tolerance mechanism that may contribute to BV recurrence and treatment failure. Our model illustrates how non-target bacteria, such as *Li* or other *Lactobacillus* spp.*,* may sequester antibiotic and lower the amount of MNZ available to target bacteria like *Gv*. The potential for non-antibiotic-target bacterial populations to act as a sink for MNZ and alter efficacy is similar to a concept that has been previously explored in bacterial ecology and termed the "the inoculum effect (**IE**)", which describes an increase in antibiotic MICs due to increased initial bacterial load and decreased per cell antibiotic concentration.[55] This model result implies that MNZ efficacy may be dependent on highly variable pre-treatment relative abundances of *Lactobacillus* spp. such as *Li* to BV-associated bacteria populations (BV:LB ratios) and raises the question of whether patients with higher levels of *Lactobacillus* spp. are more

susceptible to recurrent BV than those with higher degrees of dysbiosis. Importantly, results from the model, *in vitro* experiments, and clinical data all point to a higher pre-treatment BV-associated bacteria population relative to *Lactobacillus* spp. as a driver of MNZ efficacy in inhibiting *Gv* growth and facilitating post-treatment *Lactobacillus*-dominance. This study complements ongoing work in the search for drivers of BV treatment efficacy, in which experimental studies are often limited to delineating the role of individual bacteria, and it is challenging to assess the importance of numerous clinical and microbial variables that are associated with treatment outcome.[15]

Recent studies evaluating pre-treatment vaginal microbiota composition on MNZ efficacy have reported inconsistent results, likely due to differences in patient exclusion criteria, timepoint of treatment outcome assessment, drug regimen, and methods to collect and quantify the vaginal microbiota. One study that employed a similar drug regimen (oral MNZ) and sample collection methods to the clinical cohorts evaluated here supported our results, finding higher pre-treatment loads of antibiotic-target species, *Gv* and *A. vaginae,* associated with BV treatment efficacy.[19] Other studies that used different sample collection methods and antibiotic regimens did not explicitly evaluate the pre-treatment ratio of BV-associated bacteria to *Lactobacillus* spp.; generally suggested there was an association between total *Lactobacillus* relative abundance and successful treatment.[15,54,56] Notably, some of these studies focused on analyzing treatment outcome immediately after antibiotic therapy was completed, and in some cases treatment failure was due to no response to therapy. We propose that recurrence and failure to respond to therapy likely arise from different factors, where recurrence is due to a collective bacterial population's resilience to antibiotic therapy and failure to respond is due to inherent

resistance of BV-associated bacteria. Studies that have associated higher *Gv* loads with treatment failure correspond with the latter and could be due to the formation of biofilms or other resistance mechanisms.[56] As our model predicts immediate post-therapy *Lactobacillus* spp. relative abundance, no response to treatment would be equivalent to predicting no change or low *Lactobacillus* spp. relative abundance at 48h. An additional limitation of our model is that it does not appear to be applicable to cases of MNZ treatment failure in women who initially had very low levels of *Lactobacillus* sp. (<1%), which our model would predict should promote MNZ efficacy.[34] However, we propose that treatment failure in this case may be a result of the Allee effect,[62,63] which can be caused by a variety of mechanisms that lead to decreased fitness at low population densities, suggesting these women have *Lactobacillus* abundances that are too low to recolonize the vagina and may be associated with more precisely modeling inter-species interactions. Moreover, since *Li* is the only *Lactobacillus* sp. observed to date to significantly sequester MNZ, it will be important to characterize how other vaginal bacterial species interact with MNZ to further explore the role of non-target bacterial species on MNZ efficacy. Altogether, conflicting results in clinical studies of pre-treatment vaginal microbiota composition support the need for the development of quantitative platforms to evaluate the interplay between multiple microbial species, clinical variables, and dosing regimens that contribute to personalized differences in treatment failure.

Models presented here are only simple reconstructions of the minimal possible interactions between bacterial species and an antibiotic that have been established as key species by the existing literature[10,15,17], with a time-scale that was limited by *in vitro* co-culture conditions. While the model provided striking insight into how non-target

bacterial species may influence BV recurrence after MNZ treatment, predicting regrowth of *Lactobacillus* spp., and the full quantitative mechanisms underlying responses to treatment are likely more nuanced. More complex model frameworks did suggest key results would hold true in microbial communities with additional microbial species, interspecies interactions, and strain variability, though we were not able to validate this experimentally. Interspecies interactions in our models were incorporated with generalized Lotka-Volterra equations which simplifies relationships to a single term, but represent a good starting point for recapitulating ecosystem-level complexities.[57,58,59–61] Specific metabolic interactions that dictate survival and elimination of bacterial species in the vagina could be included with greater mechanistic detail in the future. In instances where parameters are unknown or difficult to measure experimentally, this work demonstrates the value of a global computational sensitivity analysis for understanding the relative importance of strain-level differences in antibiotic uptake, metabolism, or sensitivity. Predictive simulations can be run across multiple possible parameter ranges to determine the effects of variation prior to costly experimental measurements. This tool will be valuable in isolating the role of individual parameters in making a bacterial population or community more tolerant to antibiotic therapy.

In this study we demonstrated that ODE models can provide insights into antibiotic-microbe interactions pertinent to understanding BV treatment efficacy. Our work highlights that it is possible for BV treatment to fail, even if target bacteria are not resistant to MNZ as vaginal bacterial populations as a whole can be resilient to antibiotic, resulting in recurrent BV. While our clinical analysis is limited in sample size and therefore should be considered preliminary, future extensions of this work could be used to inform clinical

decision-making regarding personalized therapy options. More generally, we envision that the use of quantitative models such as this will provide a framework for integrating knowledge of interactions between multiple bacterial species and drug treatments in mucosal tissues to give new insight into the diverse responses observed in infectious disease and other syndromes of the female reproductive tract.

Methods

Bacterial Strains and Culture Conditions

Lactobacillus iners ATCC 55195 and *Gardnerella vaginalis* ATCC 14018 (group C) were obtained from the American Type Culture Collection (ATCC) and maintained on Human Bilayer Tween Agar (BD) plates and New York City III (NYCIII) medium according to the manufacturer's instructions. Agar plates and liquid cultures were incubated at 37°C with anaerobic gas mixture, 80% N_2, 10% CO_2, and 10% H_2. Frozen stocks of strains were stored at -80°C in 40% (v/v) glycerol.

Metronidazole Quantification by Tandem Mass Spectrometry

MNZ concentrations were determined by validated LC-MS/MS assays. Sample aliquots were centrifuged at 3000xG and divided between supernatant and cell pellet. Extracellular MNZ was extracted from supernatant via protein precipitation using acetonitrile. For intracellular concentration measurements, cell pellets were lysed using sonication and re-suspended in 100μL of sterile water. Samples were subjected to positive electrospray ionization (ESI) and detected via multiple reaction monitoring (MRM) using a LC-MS/MS system (Agilent Technologies 6460 QQQ/MassHunter). Calibration standards were

prepared with an inter- and intra-day precision and accuracy of ≤5% with an r^2 value of 0.9988±0.0009. Quantification was performed using MRM of the transitions of m/z 172.2→128.2 and 176.2 → 128.2 for MNZ and MNZ-d4 respectively. Each transition was monitored with a 100-ms dwell time. Stock solutions of MNZ and MNZ-d4 were prepared at 1mg/mL in acetonitrile-water and stored at -20°C. Mobile phase A is 0.1% acetic acid in H_2O and mobile phase B is 0.1% acetic acid in ACN, and chromatographic separation was achieved using a gradient elution with a Chromolith Performance RP-C18 column maintained at 25°C from 0-4.6 minutes, B% 0-100, with 0.5μL/min flow. During pre-study validation, calibration curves were defined in multiple runs on the basis of triplicate assays of spiked media samples as well as QC samples. This method was validated for its sensitivity, selectivity, accuracy, precision, matrix effects, recovery, and stability. Replicates of reference samples were included every 6 samples and evenly distributed throughout the MS analysis to monitor consistency and performance and to utilize for downstream normalization.

Bacterial Quantification

Bacterial quantification determined via turbidimetry was completed by measuring the optical density at each time point, 100 μL of sample inoculum was read at O.D. 600nm using a SpectraMax Plus 384 UV spectrophotometer. Time points were recorded within 5 minutes of sampling and stored at 4°C.

Bacterial quantification using plate counting was done by doing a 10-fold dilution using sterile water and aliquoting 100 μL spread evenly onto BD agar plates. Cultures were incubated at 37°C. Plating was done in triplicates and were counted manually. Prior

optimization ensured the dilution would result in no more than 300 colonies making quantification as accurate as possible.

For co-culture validation experiments, 100uL of sample was aliquoted on Rogosa agar and *Gardnerella* selective agar. Experiments were conducted to verify absence of Lactobacillus growth on *Gardnerella* selective media and absence of *G.* vaginalis growth on Rogosar agar, to confirm that colony formation specific to respective taxa. Cultures were incubated at 37°C, with a total of 36 biological replicates for the 1,000x and 0.001 Gv:Li ratio cultures (n = 18 cultures for each ratio). Plating was done in triplicates and were counted manually. Prior optimization ensured the dilution would result in no more than 300 colonies making quantification as accurate as possible.

Bacteria-MNZ experiments

For the MNZ experiments, 50μL MNZ was added at appropriate concentrations to 5mL of NYCII media. Samples equilibrated at 37°C for 1 hour prior to the addition of 50uL of bacterial inoculum ($2x10^6$). 150μL aliquot was taken for time point readings for MNZ and bacterial quantification (as described above). Samples were incubated at 37°C under constant mixing and only removed for time point measurements.

For the co-culture experiments, Gv:Li ratios were added at appropriate experimental conditions in a like-wise manner. For each varying ratio sample within each experiment, a side-by-side duplicate was performed without MNZ as a negative control. The negative control was assessed only for bacterial quantification to ensure that no growth condition or external stimuli promoted the growth of one over another. Negative control experiments demonstrated bacterial proliferation that modelled growth curves of each individual

bacterium cultured alone thus confirming any changes in growth seen in our bacteria-MNZ experiments were the result of the addition of MNZ.

ODE Models.

The model equations were constructed assuming both *Li* and *Gv* internalize MNZ at rates $k_{int\text{-}Li}$ and $k_{int\text{-}Gv}$, MNZ toxicity to *Li* and *Gv* occurred at rates dependent on the maximum rates $k_{kill\text{-}Li}$ and $k_{kill\text{-}Gv}$ and the concentration of internalized MNZ where growth inhibition increased as internalized MNZ exceeded a threshold as described by 50% effective concentrations, $EC50_{Li}$ and $EC50_{Gv}$. The growth of Li and Gv was assumed to be logistic in behavior at rates $k_{grow\text{-}Li}$ and $k_{grow\text{-}Gv}$ with distinct carrying capacities for each bacterium, K_{Li} and K_{Gv} The parameters for $k_{grow\text{-}Li}$, $k_{grow\text{-}Gv}$, K_{Li} and K_{Gv} were determined by nonlinear least squares fitting of the logistic function to growth curves for *Li* and *Gv* grown in separate cultures (fig. S2a & b).[65] The $k_{kill\text{-}Li}$, $k_{kill\text{-}Gv}$, $EC50_{Li}$ and $EC50_{Gv}$ where determined by fitting the Hill equation to kill curves for Li and Gv cultured in isolation (fig. S2c-e). Internalization rates, $k_{int\text{-}Li}$ and $k_{int\text{-}Gv}$ and metabolism rates, k_{acet} and k_{met} were determined from fitting the ODE model to time course mass spectrometry data for external MNZ, internal MNZ and acetamide and cell densities (Optical density) using a multi-start local optimization strategy (*Multistart*) with the local solver *lsqcurvefit*.

Model Simulations and Validation.

Unless otherwise noted, all simulations were completed at MNZ concentration of 500 μg/ml over the course of 48h. Growth outputs were normalized to the maximal growth density (K_{Li} and K_{Gv}) for comparison across simulations and to experimental data. External MNZ, internal MNZ and acetamide concentrations were relative to the total

volume of cellular pellet. Sensitivity analyses were completed by perturbing a single model parameter while keeping the rest of the parameters constant over 1,000x-0.001x the original value. Surfaces were generated over three orders of magnitude for MNZ concentration (10 – 1,500 μg/ml) and eight orders of magnitude for ratio of *Gv:Li* ($1.6x10^{-4}$ – $1.6x10^{4}$) at 1225 combinations of MNZ concentration and *Gv:Li* ratio. Model validation was completed by comparing the experimental co-culture data to model predictions using unpaired t-tests.

Generalized Models, inter- and intra-Species Variability and Global Sensitivity Analysis

To incorporate intraspecies and interspecies variation we developed three additional model structures and ran simulations with randomized parameter sets to determine if the influence of initial Gv:Li ratio, or the more generalized BV:LB ratio, on endpoint *Lactobacillus* spp. composition is consistently observed across these model structures.

For capturing intraspecies variation, we used Latin Hypercube Sampling of parameter ranges for each parameter to create 100 parameter sets. We derived these parameter ranges from the literature and a summary of these ranges can be found in Table S2 and Table S3. These same parameter ranges and sampling method were used for the global sensitivity and uncertainty analysis, which analyzed the partial rank correlation coefficient with 2,000 randomly generated parameter sets with endpoint (48h, 500 μg/ml MNZ) *Lactobacillus* spp. relative abundance (Marino et al., 2008).[66] For capturing interspecies variation, and microbe-microbe interactions like cross-feeding, we developed a four species model that includes two representative BV-associated bacteria, and two

494 *Lactobacillus* species, *L. iners* and a second species representing *L. crispatus, L. jensenii,*
495 or *L. gasseri.*

496 Internalization/Uptake Rates (k_{int}): To our knowledge, this is the first publication that
497 demonstrates that *G. vaginalis* and *L. iners* uptake or sequester MNZ. Previous literature
498 describing uptake of MNZ in other bacterial species, including both obligate and
499 facultative anaerobes has been published by Ralph and Denise Clarke (1978), Tally et al
500 (1978) and Narikawa (1986).[27,31,67] These publications demonstrate that even bacteria
501 that are resistant to MNZ can still uptake MNZ, and at similar rates. Despite the fact that
502 facultative anaerobes are believed to be largely insensitive to MNZ, Narikawa specifically
503 demonstrates that nitroreductase activity is associated with the ability to uptake MNZ, and
504 that pyruvate:ferrodoxin activity is associated with sensitivity to MNZ as an explanation
505 for why the facultative anaerobes *Escherichia coli, K. pneumoniae, M. morganii* and *S.*
506 *faecalis* exhibited high MICs, but reduced supernatant MNZ. We calculated the rates of
507 MNZ uptake for five species, one obligate anaerobe, *B. fragilis,* and four facultative
508 anaerobes (*E. coli, S. aureus, P. morganii and S. faecalis*) by digitizing the kinetic data
509 for cell counts and extracelluar MNZ concentrations in Ralph and Denise Clarke (1978)
510 and fitting second order reaction kinetics by ordinary least squares regression. The rates
511 ranged from $2x10^{-17}$ to 0.15 cell density$^{-1}h^{-1}$. To determine the likelihood that these
512 parameters could be a basis for *Lactobacillus* spp. uptake of MNZ, we assessed the
513 similarity between *E.* coli's oxygen independent NADPH-nitroreductase, nsfA, with
514 nitroreductase protein sequences of *G. vaginalis* (34.7%), *L. crispatus* (31.0%)*, L. iners*
515 (29.4%)*, L. jensenii* (19.4%) and *L. gasseri* (18.52%)*.* Additionally, Guillen et al (2009)
516 reported that *L. plantarum* had selective nitroreductase activity, that shared 32-43%

517 sequence similarity with several *Lactobacillus* species, and in comparison had similarity
518 with *G. vaginalis* (24.0%), *L. crispatus* (38.5%), *L. iners* (25.5%), *L. jensenii* (52.8%) and
519 *L. gasseri* (30.0%).[68] Sequence similarity was assessed by NCBI's protein BLAST.[69] As
520 obligate anaerobes were observed to uptake MNZ at higher rates, we assumed that the
521 other BV-associated bacteria, which could be an obligate anaerobe could potentially have
522 higher capacity to internalize MNZ.

523 Growth Rates (k_{grow}) and Carrying Capacities (K): To take into account potential variability
524 in growth rates, we surveyed previously published to determine ranges in growth. For
525 *Lactobacillus* species, we calculated growth rates by digitizing growth curves from
526 Chetwin et al (2019) and analyzed growth rates reported in Tomas (2003), Anukam and
527 Reid (2008). *G. vaginalis* and other bacterial strains growth curves were less abundant in
528 the literature, but we did calculate growth rates from Atassi et al., 2019 and Anukam and
529 Ried (2008).[45,49,70,71] Generally, *G. vaginalis* and other BV-associated bacteria seemed to
530 have slower growth rates than *Lactobacillus* species, and in the same culture conditions
531 this was observed in Anukam and Ried (2008). For carrying capacity we assumed that
532 there were similar carrying capacities for all species, except the BV-associated bacteria
533 based on data from Castro et al 2020, that reported *A. vaginae* at lower levels that *G.*
534 *vaginalis* at steady state.[72]

535 Sensitivity to MNZ (EC50 and k_{kill}): MNZ is highly variable, and typically obligate
536 anaerobes are considered the most sensitive to MNZ. The strain of *G. vaginalis* used in
537 the basis of this model is relatively resistant to MNZ, with growth barely inhibited at 256
538 μg/ml (9% inhibition compared to 0 μg/ml control, Fig. S2). For *A. vaginae*, the MIC can
539 range 2 ug/ml – 256 ug/ml and G. vaginalis can range from 0.75 μg/ml to > 500 μg/ml.[43,44]

Generally, it is assumed that *Lactobacillus* spp. are insensitive to MNZ; however, this also appears to be highly strain and species dependent with some Lactobacillus isolates in similar ranges of sensitivity as *G. vaginalis*.[42,45] The rate at which MNZ inhibits growth is more difficult to find, as the experiments to determine this rate are more laborious than the standard kill curve to calculate EC50 so we assumed all kill rates to be equal across all species.

Metabolism of MNZ: To our knowledge, this is the first manuscript to describe the metabolism of MNZ by vaginal microbiota. We solely based the parameter value on the rate observed for the *G. vaginalis* strain from the model. Additionally, we assumed that only BV-associated bacteria metabolism MNZ based on the observation that only BV-associated bacteria metabolize HIV microbicide drugs.[29]

Inter-species Interaction Terms: Gause (1934) first noted the calculation for interaction terms for a generalized Lotka-Volterra model describing competitive exclusion (equation 1 and 2). In our model, we generalized the interaction terms further to be able to capture many different interactions, specifically amensal behavior where *Lactobacillus* spp. can inhibit BV-associated bacterial growth with no effect of BV-associated bacteria on *Lactobacillus* species growth (-/0) as well as mutualistic (both species benefit from the other +/+) and commensal behaviors (one species benefits 0/+) between BV-associated bacteria or within the *Lactobacillus* population. The amensal behavior between *Lactobacillus* species has been documented experimentally in co-culture (Jackman et al., 2019) and we calculated the interaction term for many different species and strains of *Lactobacillus* on *G. vaginalis* and *Prevotella bivia* from Atassi et al. (2006).[50,73] It is largely believed that D-lactic acid produced by many *Lactobacillus* species inhibits the growth of

BV-associated bacteria; however, *L. iners* does not produce this isomer of lactic acid and is the reasoning behind not including an interaction term between *L. iners* and the BV-associated bacteria.[48,74] It is believed that commensal behavior exists between *G. vaginalis* and *P. bivia* in the form of cross-feeding, so we allowed the model to simulate this behavior.[51] Additionally, *G. vaginalis* is associated with promoting the growth of other BV-associated bacteria like *A. vaginae*.[72] Calculations were completed assuming the reported mono and co-cultures were at steady state to derive equation 3 and 4. Equations 2 and 3 relate to the parameter table S3 in equations 5 and 6, which generalizes the reported interaction strength from the literature to be able to be adjusted for varying carrying capacities simulated in the model that do not equal the carrying capacities from the literature.

$$1.\frac{dN}{dt} = r_{\mathrm{N}}N\left[1 - \frac{\mathrm{N} + \boldsymbol{s_{\mathrm{P}\to\mathrm{N}}}P}{K_{\mathrm{N}}}\right] \qquad 2.\frac{dP}{dt} = r_{\mathrm{P}}P\left[1 - \frac{P + \boldsymbol{s_{\mathrm{N}\to\mathrm{P}}}\boldsymbol{N}}{K_{\mathrm{P}}}\right]$$

$$\mathbf{3.}\ \boldsymbol{s_{\mathrm{P}\to\mathrm{N}}} = \left[\frac{K_{\mathrm{N}} - \mathrm{N}}{P}\right] \qquad \mathbf{4.}\ \boldsymbol{s_{\mathrm{N}\to\mathrm{P}}} = \left[\frac{K_{\mathrm{P}} - \mathrm{P}}{N}\right]$$

$$\mathbf{5.}\ \boldsymbol{s_{\mathrm{P}\to\mathrm{N}}} = \left[\frac{K_{\mathrm{N}} - \boldsymbol{f_{\mathrm{P}\to\mathrm{N}}}K_{\mathrm{N}}}{K_{\mathrm{P}}}\right] \qquad \mathbf{6.}\ \boldsymbol{s_{\mathrm{N}\to\mathrm{P}}} = \left[\frac{K_{\mathrm{P}} - \boldsymbol{f_{\mathrm{N}\to\mathrm{P}}}K_{\mathrm{P}}}{K_{\mathrm{N}}}\right]$$

Software. Parameterization, ODE modeling, sensitivity analyses, and PLSDA were completed using Matlab® 2018b (Matlab, Natick, MA). Statistical analyses were performed using PRISM 8.

Clinical data and study population

The UMB-HMP cohort: The study results and associated clinical data were previously published (Ravel et al., 2013) and all data provided was de-identified to this study. The

original clinical study protocol was approved by the Institutional Review Board of the University of Alabama at Birmingham and the University of Maryland School of Medicine. Written informed consent was appropriately obtained from all participants, who also provided consent for storage and used in future research studies related to women's health. A total of 135 nonpregnant women of reproductive age were enrolled in a longitudinal study at the University of Alabama at Birmingham. Vaginal microbiota data was generated by sequencing the V3-V4 regions of the 16S rRNA gene and is available at in dbGAP BioProject PRJNA208535.

Women self-collected cervicovaginal swabs for 10 weeks. The vaginal microbiota composition data, previously established by sequencing of the V3-V4 regions of the 16S rRNA gene, from 11 women who experienced BV (one week twice daily 500 mg oral MNZ) and were treated during the UMB-HMP study were analyzed. Any participants who failed to complete the MNZ regimen, who did not have BV according to Nugent scoring at the time of MNZ treatment, or who did not have follow-up data available were excluded from the analysis. The initial ratios of Gv:Li relative abundances were averaged across the week before starting MNZ treatment. Patients were classified to have recurrent BV if they exhibited a second episode of BV based on Nugent scoring (7-10) during remaining of the 10-week observation period.

The CONRAD BV cohort: The study results and associated clinical data were previously published (Thurman et al., 2015) and all data provided was de-identified to this study. The original clinical study protocol was approved by the Chesapeake Institutional Review Board (IRB) (Pro #00006122) with a waiver of oversight from the Eastern Virginia Medical School (EVMS) and registered in ClinicalTrials.gov (#NCT01347632). A total of 69

607 women were screened from symptomatic discharge and 35 women were enrolled in the
608 study. Vaginal microbiota data was generated by sequencing the V4 region of the 16s
609 rRNA gene, providing taxonomic resolution at the genera level.

610 Thirty-three women completed all three visits. BV was evaluated by vaginal microbiota
611 compositional data (molecular-BV).[64] After biological samples were obtained at visit 1
612 (V1), women with BV were prescribed twice daily, 500-mg MNZ for 7 days. Participants
613 returned for visit 2 (V2) 7-10 days after completing the course of MNZ therapy and visit 3
614 (V3) 28-32 days after completing treatment. At all three visits samples were obtained to
615 evaluate vaginal semen (ABAcard, West Hills, Ca), vaginal pH, gram stain for Nugent
616 score and semiquantitative vaginal flora culture. CVLs were collected, followed by vaginal
617 swabs and three full-thickness biopsies.

618 *Analysis of Clinical Outcomes.*

619 In the Human Microbiome Project cohort, patients were defined as cured or recurrent
620 based on whether after initial MNZ treatment the patient suffered an additional episode
621 of BV (Nugent 7-10) during the 10-week course of data collection. For analysis, initial flora
622 relative abundances were averaged across the 7 days prior to reported treatment start
623 date. To analyze the relative ratio between BV-associated bacteria and *Lactobacillus*
624 spp., we combined the relative abundances for the top twenty BV-associated bacteria
625 and all *Lactobacillus* spp. The genera BV-associated bacteria included were: *Gardnerella,*
626 *Atopobium, Megasphaera,* BVAB1-3, *Streptococcus, Prevotella, Leptotrichia,*
627 *Anaerococcus, Peptoniphilus, Eggerthella, Veillonella, Sneathia, Mobiluncus,*
628 *Corynebacterium, Ureaplasma, Eubacterium, Porphyromonas, Dialister,*
629 *Peptostreptococcus, Bacteroides, Fusobacterium, Actinomyces, Bifidobacterium*. Before

630 statistical analysis, the BV:LB ratio was log-transformed, and the relative abundances of
631 *L. iners, G. vaginalis* were center-log ratio (CLR) transformed, with pseudocounts added
632 to taxonomic units with relative abundances equal to zero, to compare between cured
633 and the recurrent groups by one-way unpaired t-tests and were corrected using the FDR
634 method of Benjamini and Hochberg (PRISM 8).

635 For the CONRAD BV cohort, treatment outcome was defined based on *Lactobacillus*
636 dominance evaluated at enrollment, 7 days after treatment and 28-32 days after
637 treatment. Patients that exhibited *Lactobacillus* dominance at both 1 week and 1 month
638 after treatment were considered cured, and patients that exhibited *Lactobacillus*
639 dominance only at week 1 and not at 1 month were considered recurrent. The statistical
640 analysis followed the same methodology as the HMP Cohort.

641 Data availability

642 Data used to parameterize and validate the model are available upon request (Fig. 2, Fig.
643 S1-S2). The UMB-HMP cohort study sequence data and metadata were deposited in the
644 Sequence Read Archive (SRA; http://www.ncbi.nlm.nih.gov/Traces/sra/) under
645 BioProject PRJNA208535 ("The daily dynamics of the vaginal microbiota before and after
646 bacterial vaginosis"; http://www.ncbi.nlm.nih.gov/bioproject/? term=PRJNA208535)
647 ([SRP026107] and [SRA091234]). An abbreviated data set necessary for the reproduction
648 of Fig. 5a-c is in Table S4. The data from the CONRAD BV study are not in a formal
649 repository, but are fully available upon request. An abbreviated data set necessary for
650 reproduction of Fig. 5d-f is in Table S5.
651

652 Code availability

653 All code is available at https://github.com/chyylee/BV.

654 **Competing Interests**

655 JR is co-founder of LUCA Biologics, a biotechnology company focusing on translating
656 microbiome research into live biotherapeutic drugs for women's health. All other authors
657 declare no competing interests.

658

659 **Authorship Contributions**

660 CYL, RKC, MML, NRK and KBA conceived and designed the study. CYL completed the
661 computational analysis and analyzed the clinical data. RKC, NRK, and BH designed and
662 conducted monoculture and co-culture kinetic experiments. AG, MF, and JR curated data
663 from the UMB-HMP cohort. JR lead the UMB-HMP study and data collection. AT and GD
664 provided CONRAD BV protocol development, patient care, and data analysis. CYL, RKC,
665 KBA, and NRK wrote the manuscript and all authors read and revised the manuscript.

666

667 **Acknowledgements**

668 This work was in part funded by startup funds from the University of Miami to NRK, funds
669 from NIH/NIDDK grant RO1DK112254 to NRK, and NIH/NIAID grant R01AI138718
670 subcontract to NRK, and startup funds from the University of Michigan to KBA. The UMB-
671 HMP study, JR and MF were supported by the National Institute for Allergy and Infectious

672 Diseases of the National Institutes of Health under award numbers UH2AI083264 and
673 R01NR015495. The CONRAD BV Study was funded by an intra-agency agreement
674 between the Centers for Disease Control and Prevention (CDC), United States Aid and
675 International Development (USAID) and CONRAD (GPO-A-00-08-00005-00). The views
676 expressed by the authors do not necessarily reflect those of the funding agency or
677 CONRAD.

References

1. Koumans, E. *et al.* The Prevalence of Bacterial Vaginosis in the United States, 2001–2004; Associations With Symptoms, Sexual Behaviors, and Reproductive Health. *Sex. Transm. Dis.* **34**, 864–869 (2007).
2. Peebles, K., Velloza, J., Balkus, J. E., McClelland, R. S. & Barnabas, R. V. High Global Burden and Costs of Bacterial Vaginosis: A Systematic Review and Meta-Analysis. *Sex. Transm. Dis.* **46**, 304–311 (2019).
3. Taha, T. *et al.* Bacterial vaginosis and disturbances of vaginal flora: association with increased acquisition of HIV. *Aids* **12**, 1699–1706 (1998).
4. Haggerty, C. L., Hillier, S. L., Bass, D. C. & Ness, R. B. Bacterial Vaginosis and Anaerobic Bacteria Are Associated with Endometritis. *Clin. Infect. Dis.* **39**, 990–995 (2004).
5. Hillier, S. L. *et al.* Association between bacterial vaginosis and preterm delivery of a low-birth-weight infant. The Vaginal Infections and Prematurity Study Group. *N. Engl. J. Med.* **333**, 1737–1742 (1995).

6. Bradshaw, C. S. & Brotman, R. M. Making inroads into improving treatment of bacterial vaginosis - striving for long-term cure. *BMC Infect. Dis.* **15**, 292 (2015).
7. Ness, R. B. *et al.* A cluster analysis of bacterial vaginosis-associated microflora and pelvic inflammatory disease. *Am. J. Epidemiol.* **162**, 585–590 (2005).
8. Nunn, K. L. & Forney, L. J. Unraveling the Dynamics of the Human Vaginal Microbiome. *Yale J. Biol. Med.* **89**, 331–337 (2016).
9. Fredricks, D. N., Fiedler, T. L., Thomas, K. K., Mitchell, C. M. & Marrazzo, J. M. Changes in Vaginal Bacterial Concentrations with Intravaginal Metronidazole Therapy for Bacterial Vaginosis as Assessed by Quantitative PCR. *J. Clin. Microbiol.* **47**, 721–726 (2009).
10. Srinivasan, S. *et al.* Temporal Variability of Human Vaginal Bacteria and Relationship with Bacterial Vaginosis. *PLOS ONE* **5**, e10197 (2010).
11. Bradshaw, C. S. *et al.* High Recurrence Rates of Bacterial Vaginosis over the Course of 12 Months after Oral Metronidazole Therapy and Factors Associated with Recurrence. *J. Infect. Dis.* **193**, 1478–1486 (2006).
12. Bradshaw, C. S. & Sobel, J. D. Current Treatment of Bacterial Vaginosis-Limitations and Need for Innovation. *J. Infect. Dis.* **214 Suppl 1**, S14-20 (2016).
13. Ma, L., Su, J., Su, Y., Sun, W. & Zeng, Z. Probiotics administered intravaginally as a complementary therapy combined with antibiotics for the treatment of bacterial vaginosis: a systematic review protocol. *BMJ Open* **7**, e019301 (2017).
14. Ferris, D. G., Litaker, M. S., Woodward, L., Mathis, D. & Hendrich, J. Treatment of bacterial vaginosis: a comparison of oral metronidazole, metronidazole vaginal gel, and clindamycin vaginal cream. *J. Fam. Pract.* **41**, 443–449 (1995).

15. Xiao, B. *et al.* Association Analysis on Recurrence of Bacterial Vaginosis Revealed Microbes and Clinical Variables Important for Treatment Outcome. *Front. Cell. Infect. Microbiol.* **9**, (2019).

16. Brotman, R. M. *et al.* A Longitudinal Study of Vaginal Douching and Bacterial Vaginosis—A Marginal Structural Modeling Analysis. *Am. J. Epidemiol.* **168**, 188–196 (2008).

17. Wang, B. *et al.* Molecular analysis of the relationship between specific vaginal bacteria and bacterial vaginosis metronidazole therapy failure. *Eur. J. Clin. Microbiol. Infect. Dis.* **33**, 1749–1756 (2014).

18. Zhou, X. *et al.* Recent Advances in Understanding the Microbiology of the Female Reproductive Tract and the Causes of Premature Birth. *Infectious Diseases in Obstetrics and Gynecology* https://www.hindawi.com/journals/idog/2010/737425/abs/ (2010) doi:10.1155/2010/737425.

19. Ferreira, C. S. T. *et al.* Treatment failure of bacterial vaginosis is not associated with higher loads of Atopobium vaginae and Gardnerella vaginalis. *J. Med. Microbiol.* **66**, 1217–1224 (2017).

20. Coleman, J. S. & Gaydos, C. A. Molecular Diagnosis of Bacterial Vaginosis: an Update. *J. Clin. Microbiol.* **56**, (2018).

21. Gajer, P. *et al.* Temporal Dynamics of the Human Vaginal Microbiota. *Sci. Transl. Med.* **4**, 132ra52 (2012).

22. Tamarelle, J. *et al.* Non-optimal vaginal microbiota after azithromycin treatment for Chlamydia trachomatis infection. *J. Infect. Dis.* (2019) doi:10.1093/infdis/jiz499.

23. Vaneechoutte, M. Lactobacillus iners, the unusual suspect. *Res. Microbiol.* **168**, 826–836 (2017).

24. Faust, K., Lahti, L., Gonze, D., de Vos, W. M. & Raes, J. Metagenomics meets time series analysis: unraveling microbial community dynamics. *Curr. Opin. Microbiol.* **25**, 56–66 (2015).

25. Lugo-Martinez, J., Ruiz-Perez, D., Narasimhan, G. & Bar-Joseph, Z. Dynamic interaction network inference from longitudinal microbiome data. *Microbiome* **7**, 54 (2019).

26. Brotman, R. M., Ravel, J., Cone, R. A. & Zenilman, J. M. Rapid fluctuation of the vaginal microbiota measured by Gram stain analysis. *Sex. Transm. Infect.* **86**, 297–302 (2010).

27. Tally, F. P., Goldin, B. R., Sullivan, N., Johnston, J. & Gorbach, S. L. Antimicrobial activity of metronidazole in anaerobic bacteria. *Antimicrob. Agents Chemother.* **13**, 460–465 (1978).

28. Church, D. L., Rabin, H. R. & Lalshley, E. J. Role of hydrogenase 1 of clostridium pasteurianum in the reduction of metronidazole. *Biochem. Pharmacol.* **37**, 1525–1534 (1988).

29. Klatt, N. R. *et al.* Vaginal bacteria modify HIV tenofovir microbicide efficacy in African women. *Science* **356**, 938–945 (2017).

30. Edwards, D. I. Mechanisms of selective toxicity of metronidazole and other nitroimidazole drugs. *Br. J. Vener. Dis.* **56**, 285–290 (1980).

31. Ralph, E. D. & Clarke, D. A. Inactivation of Metronidazole by Anaerobic and Aerobic Bacteria. *Antimicrob. Agents Chemother.* **14**, 377–383 (1978).

32. Edwards, D. I., Thompson, E. J., Tomusange, J. & Shanson, D. Inactivation of metronidazole by aerobic organisms. *J. Antimicrob. Chemother.* **5**, 315–316 (1979).

33. Ravel, J. *et al.* Daily temporal dynamics of vaginal microbiota before, during and after episodes of bacterial vaginosis. *Microbiome* **1**, 29 (2013).

34. Thurman, A. R. *et al.* Bacterial Vaginosis and Subclinical Markers of Genital Tract Inflammation and Mucosal Immunity. *AIDS Res. Hum. Retroviruses* **31**, 1139–1152 (2015).

35. Koch, R. L., Chrystal, E. J., Beaulieu, B. B. & Goldman, P. Acetamide--a metabolite of metronidazole formed by the intestinal flora. *Biochem. Pharmacol.* **28**, 3611–3615 (1979).

36. Regoes, R. R. *et al.* Pharmacodynamic functions: a multiparameter approach to the design of antibiotic treatment regimens. *Antimicrob. Agents Chemother.* **48**, 3670–3676 (2004).

37. Meredith, H. R. *et al.* Applying ecological resistance and resilience to dissect bacterial antibiotic responses. *Sci. Adv.* **4**, eaau1873 (2018).

38. Ings, R. M., McFadzean, J. A. & Ormerod, W. E. The mode of action of metronidazole in Trichomonas vaginalis and other micro-organisms. *Biochem. Pharmacol.* **23**, 1421–1429 (1974).

39. Davis, B., Glover, D. D. & Larsen, B. Analysis of metronidazole penetration into vaginal fluid by reversed-phase high-performance liquid chromatography. *Am. J. Obstet. Gynecol.* **149**, 802–803 (1984).

40. Simoes, J. A. *et al.* Human Immunodeficiency Virus Type 1 Stimulatory Activity by Gardnerella vaginalis: Relationship to Biotypes and Other Pathogenic Characteristics. *J. Infect. Dis.* **184**, 22–27 (2001).

41. Brooks, J. P. *et al.* Changes in vaginal community state types reflect major shifts in the microbiome. *Microb. Ecol. Health Dis.* **28**, (2017).

42. Simoes, J. A., Aroutcheva, A. A., Shott, S. & Faro, S. Effect of metronidazole on the growth of vaginal lactobacilli in vitro. *Infect. Dis. Obstet. Gynecol.* **9**, 41–45 (2001).

43. De Backer, E. *et al.* Antibiotic susceptibility of Atopobium vaginae. *BMC Infect. Dis.* **6**, 51 (2006).

44. Petrina, M. A. B., Cosentino, L. A., Rabe, L. K. & Hillier, S. L. Susceptibility of bacterial vaginosis (BV)-associated bacteria to secnidazole compared to metronidazole, tinidazole and clindamycin. *Anaerobe* **47**, 115–119 (2017).

45. Anukam, K. C. & Reid, G. Effects of metronidazole on growth of Gardnerella vaginalis ATCC 14018, probiotic Lactobacillus rhamnosus GR-1 and vaginal isolate Lactobacillus plantarum KCA. *Microb. Ecol. Health Dis.* **20**, 48–52 (2008).

46. Buffie, C. G. *et al.* Profound Alterations of Intestinal Microbiota following a Single Dose of Clindamycin Results in Sustained Susceptibility to Clostridium difficile-Induced Colitis. *Infect. Immun.* **80**, 62–73 (2012).

47. France, M. T., Mendes-Soares, H. & Forney, L. J. Genomic Comparisons of Lactobacillus crispatus and Lactobacillus iners Reveal Potential Ecological Drivers of Community Composition in the Vagina. *Appl. Environ. Microbiol.* **82**, 7063–7073 (2016).

48. O'Hanlon, D. E., Moench, T. R. & Cone, R. A. Vaginal pH and microbicidal lactic acid when lactobacilli dominate the microbiota. *PloS One* **8**, e80074 (2013).

49. Atassi, F., Pho Viet Ahn, D. L. & Lievin-Le Moal, V. Diverse Expression of Antimicrobial Activities Against Bacterial Vaginosis and Urinary Tract Infection Pathogens by Cervicovaginal Microbiota Strains of Lactobacillus gasseri and Lactobacillus crispatus. *Front. Microbiol.* **10**, (2019).

50. Atassi, F., Brassart, D., Grob, P., Graf, F. & Servin, A. L. Lactobacillus strains isolated from the vaginal microbiota of healthy women inhibit Prevotella bivia and Gardnerella vaginalis in coculture and cell culture. *FEMS Immunol. Med. Microbiol.* **48**, 424–432 (2006).

51. Pybus, V. & Onderdonk, A. B. Evidence for a commensal, symbiotic relationship between Gardnerella vaginalis and Prevotella bivia involving ammonia: potential significance for bacterial vaginosis. *J. Infect. Dis.* **175**, 406–413 (1997).

52. Ravel, J. *et al.* Vaginal microbiome of reproductive-age women. *Proc. Natl. Acad. Sci.* **108**, 4680–4687 (2011).

53. Deng, Z.-L. *et al.* Metatranscriptome Analysis of the Vaginal Microbiota Reveals Potential Mechanisms for Protection against Metronidazole in Bacterial Vaginosis. *mSphere* **3**, (2018).

54. Xiao, B. *et al.* Predictive value of the composition of the vaginal microbiota in bacterial vaginosis, a dynamic study to identify recurrence-related flora. *Sci. Rep.* **6**, (2016).

55. Brook, I. Inoculum Effect. *Rev. Infect. Dis.* **11**, 361–368 (1989).

56. Verwijs, M. C., Agaba, S. K., Darby, A. C. & Wijgert, J. H. H. M. van de. Impact of oral metronidazole treatment on the vaginal microbiota and correlates of treatment failure. *Am. J. Obstet. Gynecol.* **222**, 157.e1-157.e13 (2020).

57. Stein, R. R. *et al.* Ecological Modeling from Time-Series Inference: Insight into Dynamics and Stability of Intestinal Microbiota. *PLOS Comput. Biol.* **9**, e1003388 (2013).

58. May, R. *Stability and Complexity in Model Ecosystems*. (2001).

59. Medlock, G. L. *et al.* Inferring Metabolic Mechanisms of Interaction within a Defined Gut Microbiota. *Cell Syst.* **7**, 245-257.e7 (2018).

60. Momeni, B., Xie, L. & Shou, W. Lotka-Volterra pairwise modeling fails to capture diverse pairwise microbial interactions. *eLife* **6**, e25051 (2017).

61. Goldford, J. E. *et al.* Emergent simplicity in microbial community assembly. *Science* **361**, 469–474 (2018).

62. Allee, W. C. *Principles of animal ecology,*. (Saunders Co., 1949).

63. Goswami, M., Bhattacharyya, P. & Tribedi, P. Allee effect: the story behind the stabilization or extinction of microbial ecosystem. *Arch. Microbiol.* **199**, 185–190 (2017).

64. McKinnon, L. R. *et al.* The Evolving Facets of Bacterial Vaginosis: Implications for HIV Transmission. *AIDS Res. Hum. Retroviruses* **35**, 219–228 (2019).

65. McKendrick, A. G. & Pai, M. K. XLV.—The Rate of Multiplication of Micro-organisms: A Mathematical Study. *Proc. R. Soc. Edinb.* **31**, 649–653 (1912).

66. Marino, S., Hogue, I. B., Ray, C. J. & Kirschner, D. E. A Methodology For Performing Global Uncertainty And Sensitivity Analysis In Systems Biology. *J. Theor. Biol.* **254**, 178–196 (2008).

67. Narikawa, S. Distribution of metronidazole susceptibility factors in obligate anaerobes. *J. Antimicrob. Chemother.* **18**, 565–574 (1986).

68. Guillén, H., Curiel, J. A., Landete, J. M., Muñoz, R. & Herraiz, T. Characterization of a Nitroreductase with Selective Nitroreduction Properties in the Food and Intestinal Lactic Acid Bacterium Lactobacillus plantarum WCFS1. *J. Agric. Food Chem.* **57**, 10457–10465 (2009).

69. Altschul, S. F. & Koonin, E. V. Iterated profile searches with PSI-BLAST--a tool for discovery in protein databases. *Trends Biochem. Sci.* **23**, 444–447 (1998).

70. Chetwin, E. *et al.* Antimicrobial and inflammatory properties of South African clinical Lactobacillus isolates and vaginal probiotics. *Sci. Rep.* **9**, 1917 (2019).

71. Juárez Tomás, M. S., Ocaña, V. S., Wiese, B. & Nader-Macías, M. E. Growth and lactic acid production by vaginal Lactobacillus acidophilus CRL 1259, and inhibition of uropathogenic Escherichia coli. *J. Med. Microbiol.* **52**, 1117–1124 (2003).

72. Castro, J., Rosca, A. S., Cools, P., Vaneechoutte, M. & Cerca, N. Gardnerella vaginalis Enhances Atopobium vaginae Viability in an in vitro Model. *Front. Cell. Infect. Microbiol.* **10**, 83 (2020).

73. Jackman, C. M., Deans, K. W., Forney, L. J. & Lin, X. N. Microdroplet co-cultivation and interaction characterization of human vaginal bacteria. *Integr. Biol.* **11**, 69–78 (2019).

74. France, M. T., Mendes-Soares, H. & Forney, L. J. Genomic Comparisons of Lactobacillus crispatus and Lactobacillus iners Reveal Potential Ecological Drivers of Community Composition in the Vagina. *Appl. Environ. Microbiol.* **82**, 7063–7073 (2016).

FIGURES

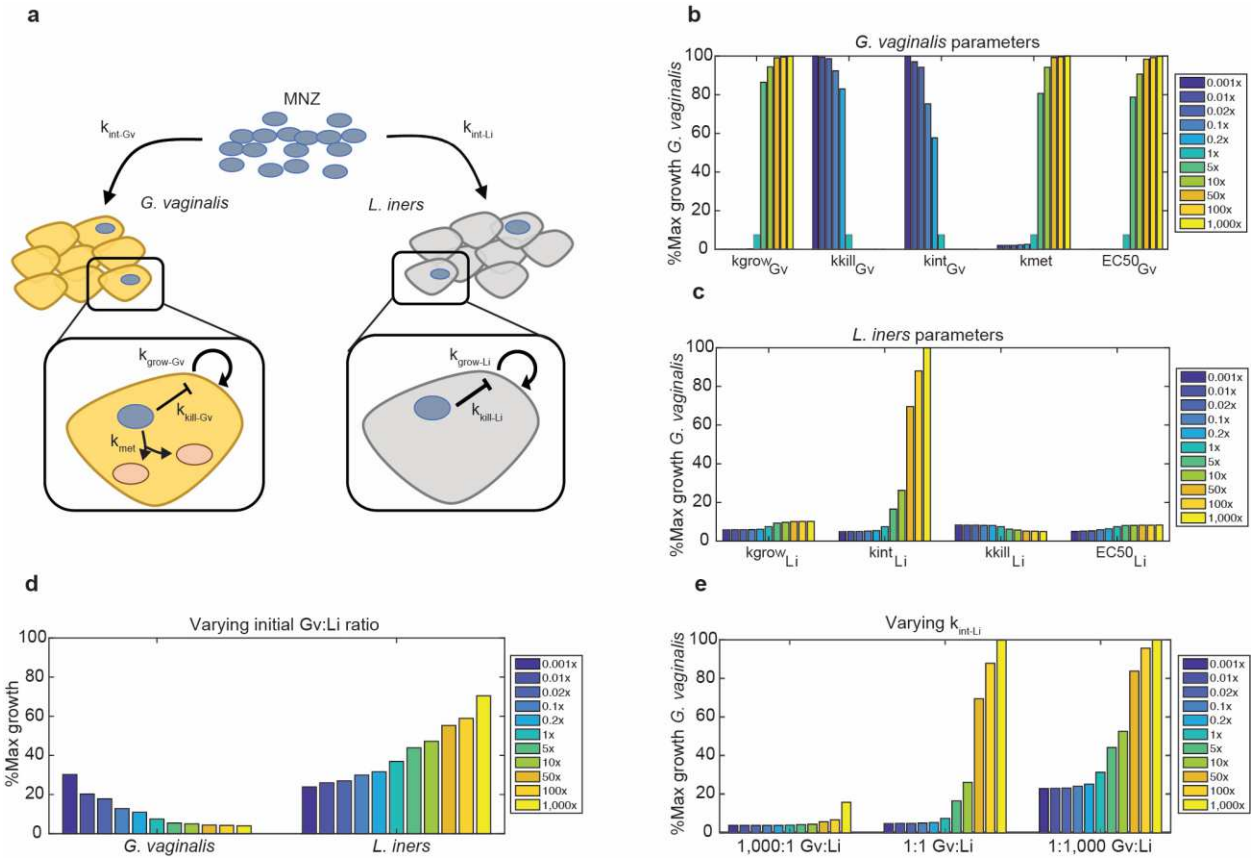

Figure 1: Model schematic for bacterial growth dynamics in BV with MNZ treatment. (a) MNZ is internalized by both *G. vaginalis* (*Gv*) and *L. iners* (*Li*) at rates k_{int-GV} and k_{int-LI}, cells are proliferating at $k_{grow-GV}$ and $k_{grow-LI}$ and MNZ inhibits growth by $k_{kill-GV}$ and $k_{kill-LI}$. For *G. vaginalis*, a potential mechanism of MNZ resistance is the bacterial-mediated interactions to the drug leading to the formation of metabolites (k_{met}). (b) Sensitivity of *Gv* growth with 500 μg/ml MNZ when parameters directly related to *Gv* growth are varied 0.001x to 1,000x baseline values. Percent maximal growth refers to the final cell count compared to the carrying capacity of the culture, or the maximum cell count the unperturbed culture can reach at 48h based on initial cell counts (c) Sensitivity of *Gv*

growth with 500 μg/ml MNZ when parameters related to *Li* survival are varied 0.001x to 1,000x baseline values. (d) Max growth of *Gv* (left) and *Li* (right) when the initial ratio of *Gv* to *Li* is varied with 500 μg/ml MNZ treatment. (e) Max growth of *Gv when* MNZ internalization rate of *Li* is varied at three different population compositions with 500 μg/ml MNZ treatment.

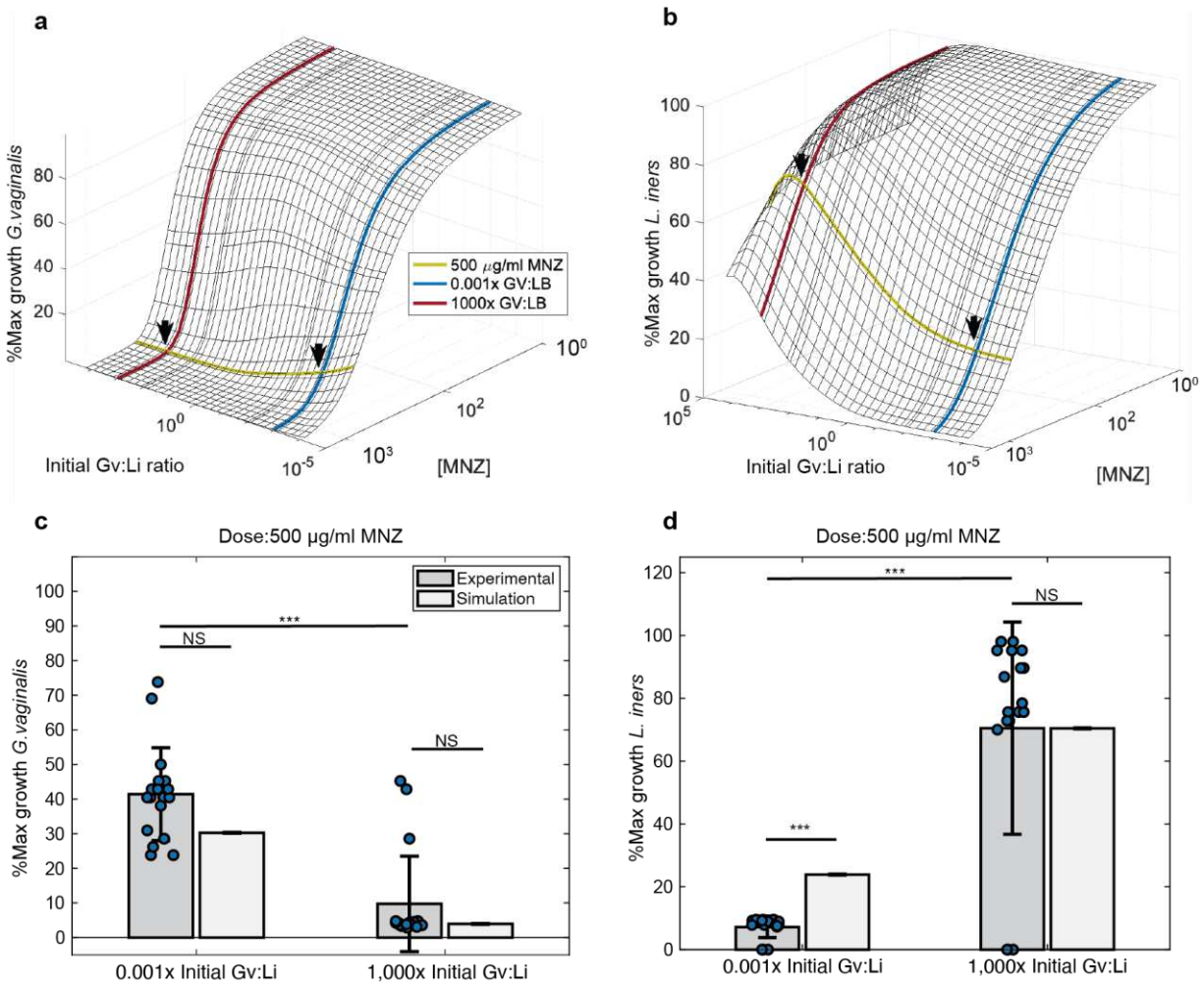

Figure 2: A higher initial Gv:Li ratio improves MNZ treatment efficacy. (a) Surface plot to illustrate predicted percent maximal growth of *Gv* (z-axis) when concentration of MNZ (x-axis) and the ratio of Gv:Li (y-axis) are varied in simultaneously. Arrows indicate the concentration of MNZ and ratios of Gv:Li used for model validation. (b) Percent maximal growth of *Li* after simultaneous variation of MNZ dose and Gv:Li ratio. (c-d) Comparison of model simulations to experimental data for 500 μg/ml MNZ at 1000x and 0.001x Gv:Li (* $p < 0.05$, ** $p < 0.01$, *** $p < 0.001$, unpaired two-tailed t-test, error bars represent standard deviation).

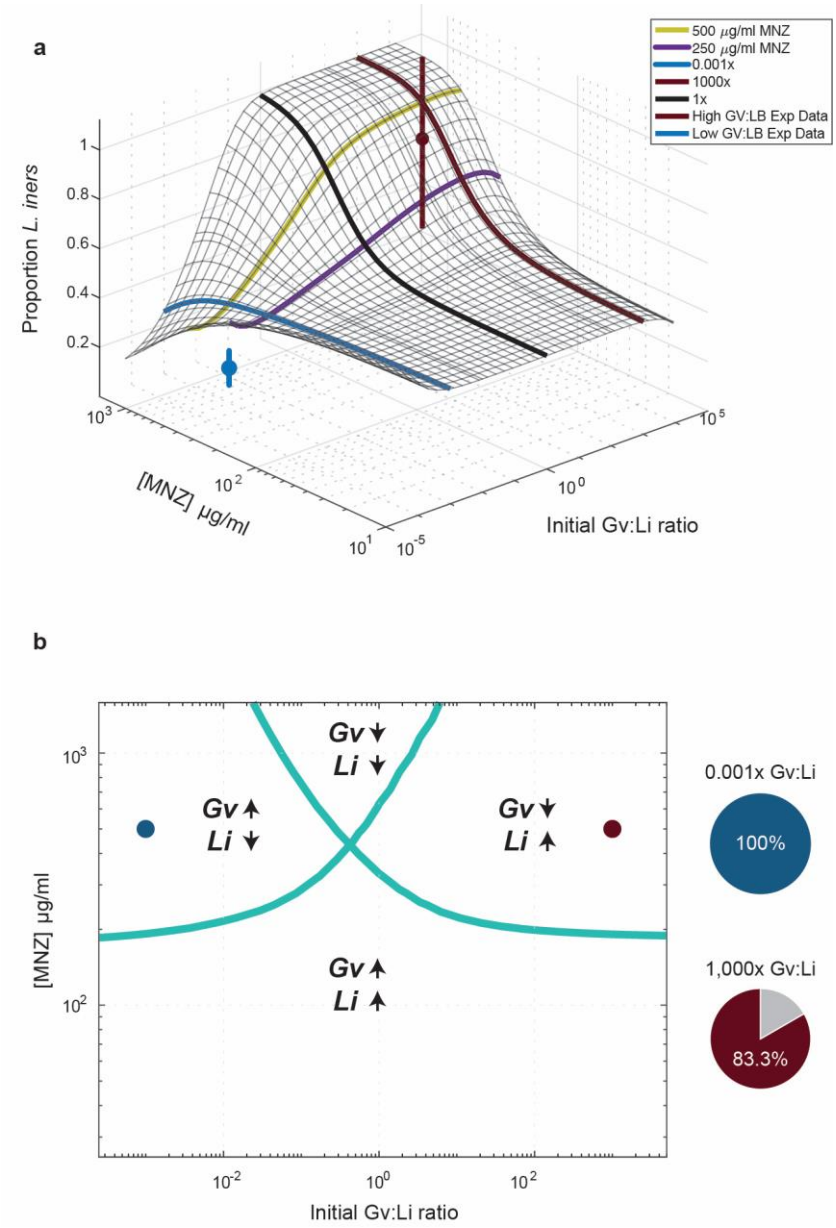

Figure 3: Initial Gv:Li ratios dictate final microbial populations. (a) Surface plot illustrates model predictions for proportion of *Li* relative to *Gv* 48h at different starting Gv:Li ratios (x-axis) and at different doses of MNZ (y-axis). Experimental validation was performed in in vitro co-cultures of Li and Gv (n = 36) and is plotted on the surface, with mean and ± standard deviation represented by nodes and vertical lines (b) Phase diagram of microbial growth dynamics 48hrs after exposure to various MNZ doses, dots indicate experimental conditions evaluated. There are four possibilities: Both *Gv* and *Li*

populations are increased after treatment, both *Gv* and *Li* populations are decreased, only the *Gv* population is increased and only the *Li* population is increased. Pie charts indicate the fraction of experimental samples that agree with the predicted trends (right).

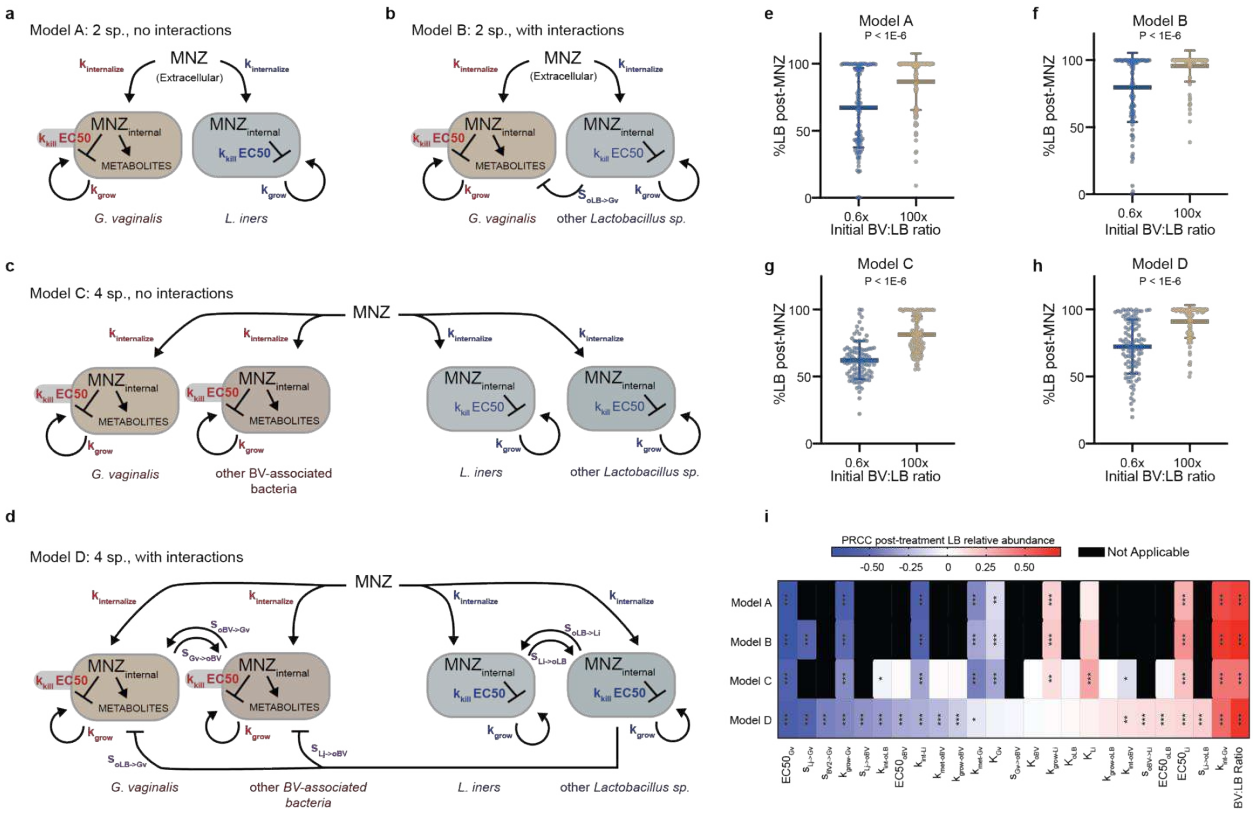

Figure 4: High pre-treatment BV:LB ratio is predicted to reduce MNZ efficacy in more complex microbial environments regardless of strain variability. (A) Original model structure validated in Fig. 2 (B) Two species model with negative interaction between other *Lactobacillus* sp. (oLB) and *Gv* (c) Four species model of *Gv* and *Li* with additional representative bacteria for BV-associated bacteria and *Lactobacillus* sp. (d) Four species model with inter-species interactions. Within BV-associated bacteria and *Lactobacillus* sp. interactions were simulated from mutualistic (both benefit) to commensal (one benefits, the other is neutral). Inhibitory (amensal) interactions are included between D-lactic acid producing bacteria, other *Lactobacillus sp.,* with both BV-associated bacteria (e-h) post-MNZ treatment (48h, 500 μg/ml) *Lactobacillus* sp. relative abundances at. 0.6x and 100x BV-associated bacteria to *Lactobacillus* sp (BV:LB) ratios.

Each point represents a parameter set randomly sampled from physiological ranges in Tables S2 and S3 (i) Significantly sensitive parameters (assessed by partial rank correlation) for each model structure (a-d) as determined by the global sensitivity and uncertainty analysis.

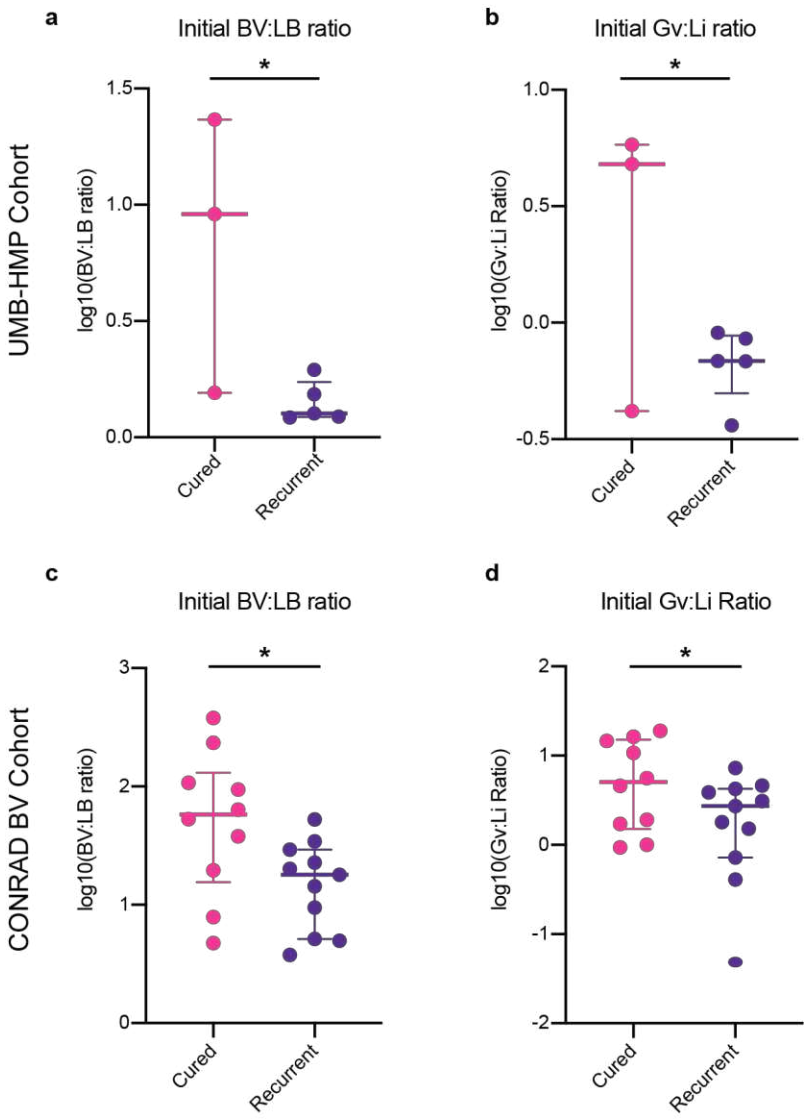

Figure 5: Increased initial BV:LB ratios associated with successful treatment of BV. (a – b) clinical results for the UMB-HMP cohort describing the (a) log base 10 transform of initial BV-associated bacteria relative abundance to *Lactobacillus* sp. relative abundance (b) initial Gv:Li ratio. (c – d) Clinical results for the CONRAD BV cohort (c) log base 10 transform of initial BV-associated bacteria relative abundance to *Lactobacillus* sp. relative abundance. (d) initial Gv:Li ratio. Lines depict the 25th, 50th and 75th percentiles, multiple unpaired one-tailed t-test p-values were adjusted using Benjamini and Hochberg correction.

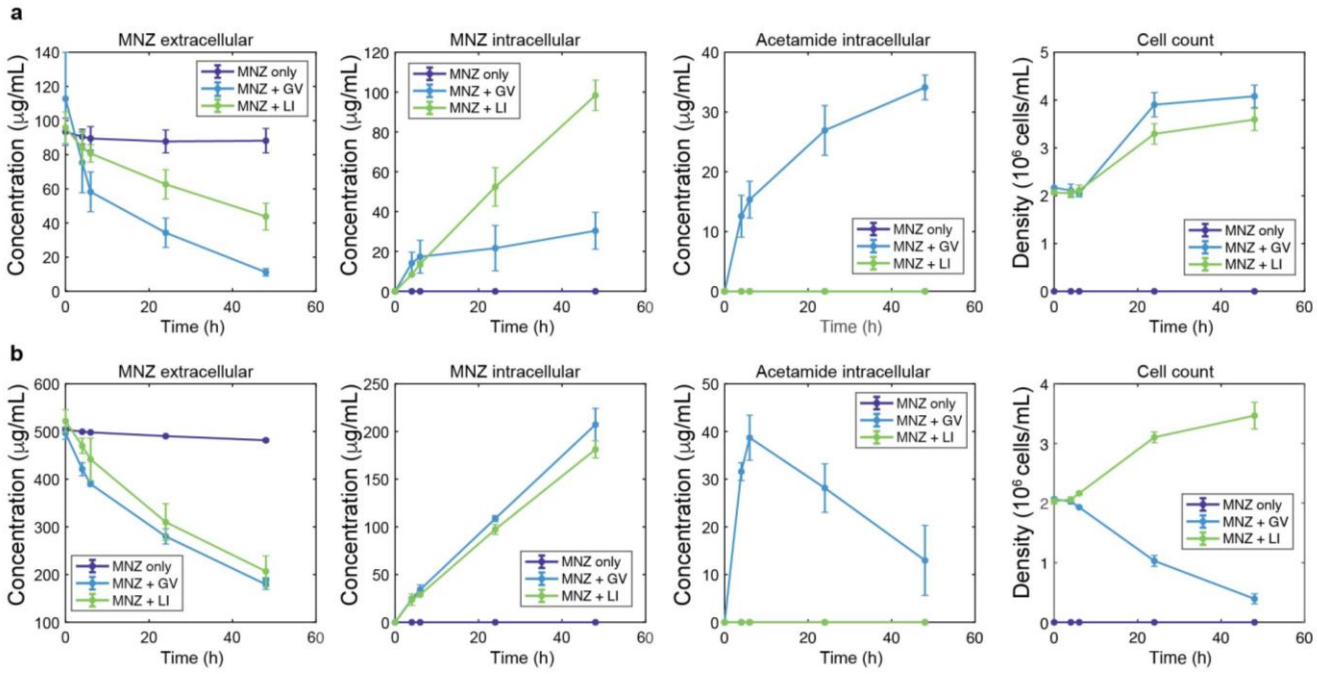

Supplementary Figure 1: Kinetic data for parameterization of MNZ interactions with *L. iners* and *G. vaginalis*. Kinetic data was collected at two doses of MNZ, (a) low dose (100 μg/ml) and (b) high dose (500 μg/ml) for cultures with only MNZ, *Gv* and *Li* treated with MNZ (error bars ± SD).

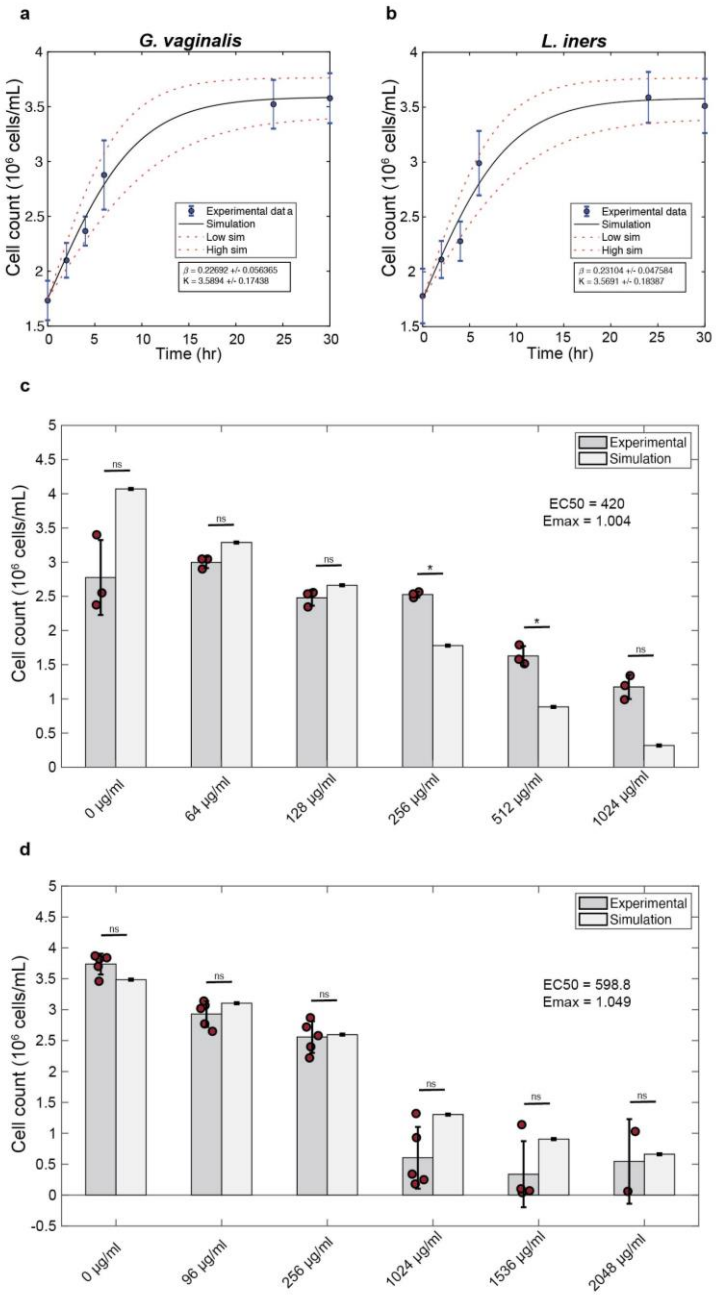

Supplementary Figure 2: Model parameterization of growth dynamics with and without MNZ. (a-b) growth curves fit to a logistic equation using least-squares regression, growth rates and carrying capacity was determined from this data. Red dashed lines represent confidence interval, values represent mean ± SD (c-d) Kill curves used to determine the maximal kill rate and EC50 of MNZ for *Gv* and *Li*.

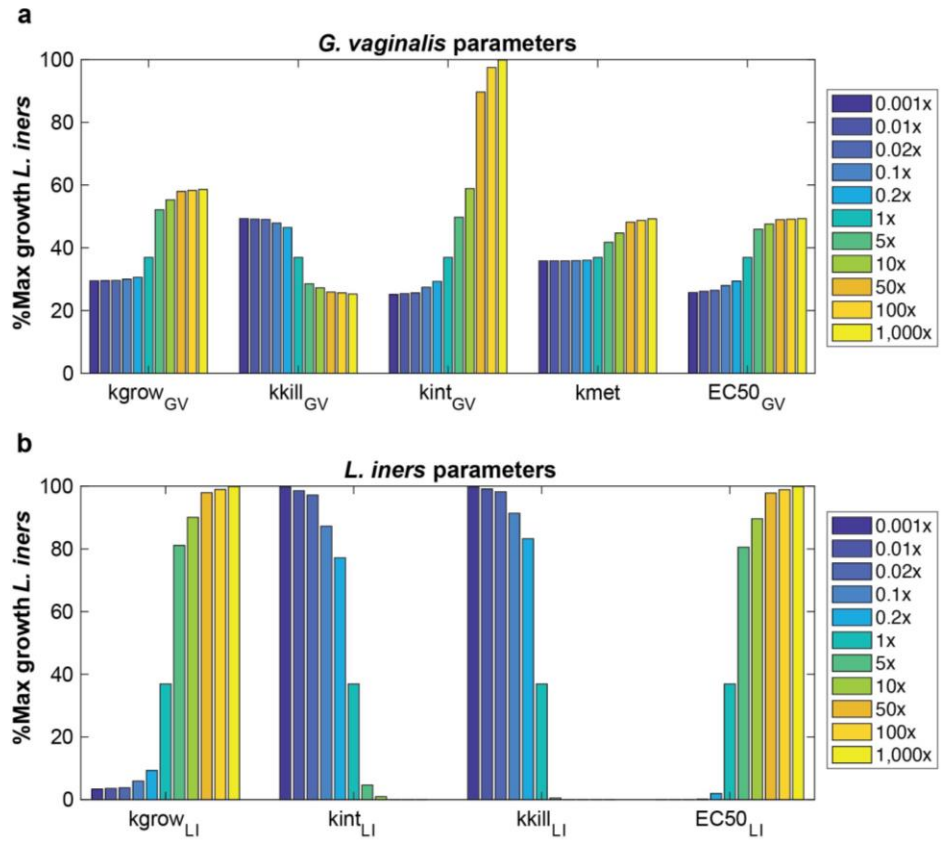

Supplementary Figure 3*: L. iners* 1D sensitivity analysis. (a) Sensitivity of *Li* growth with 500 μg/ml MNZ when parameters directly related to *Li* growth and survival are varied 0.001x to 1,000x fold baseline values. Percent maximal growth refers to the final cell count compared to the carrying capacity of the culture, the maximum cell count the culture can reach (b) Sensitivity of *Li* growth with 500 μg/ml MNZ when parameters related to *Li* survival are varied 0.001x to 1,000x fold baseline values.

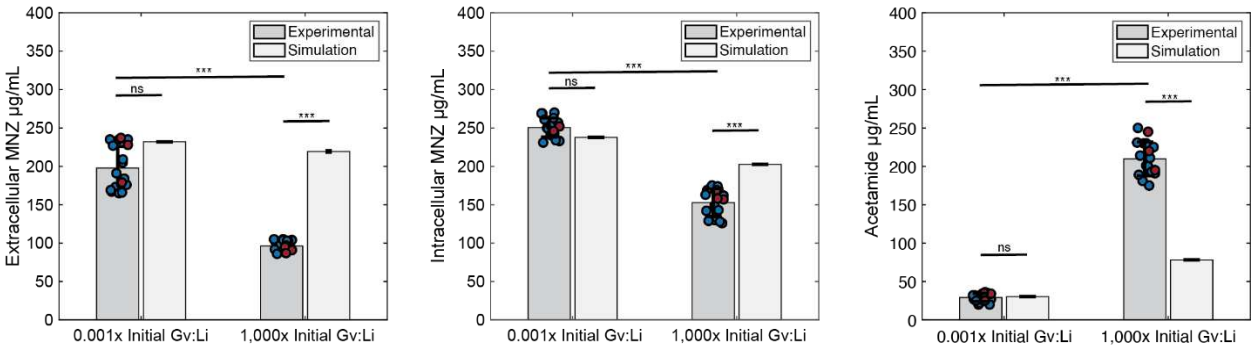

Supplementary Figure 4: Model validation. Validation for the model for extracellular MNZ, intracellular MNZ and acetamide. Intracellular MNZ is the sum of MNZ concentration in *Li* and *Gv* in the model (* $p < 0.05$, ** $p < 0.01$, *** $p < 0.001$, unpaired two-tailed t-test, error bars represent standard deviation).

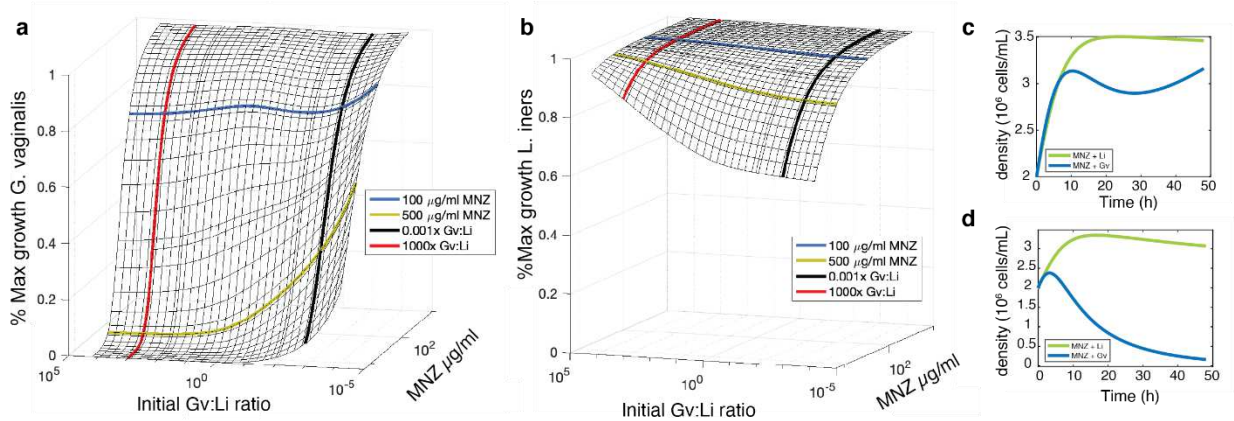

Supplementary Figure 5: *L. iners* susceptibility to MNZ does not influence Gv:Li ratio dependent MNZ efficacy. (a - b) Surface plot to illustrate predicted percent maximal growth of (a) *Gv* and (b) *Li* (z-axis) when concentration of MNZ (x-axis) and the initial ratio of Gv:Li (y-axis) are varied in simultaneously. (c – d) Model predicted growth dynamics for monoculture response to MNZ at (c) 100 µg/ml and (d) 500 µg/ml.

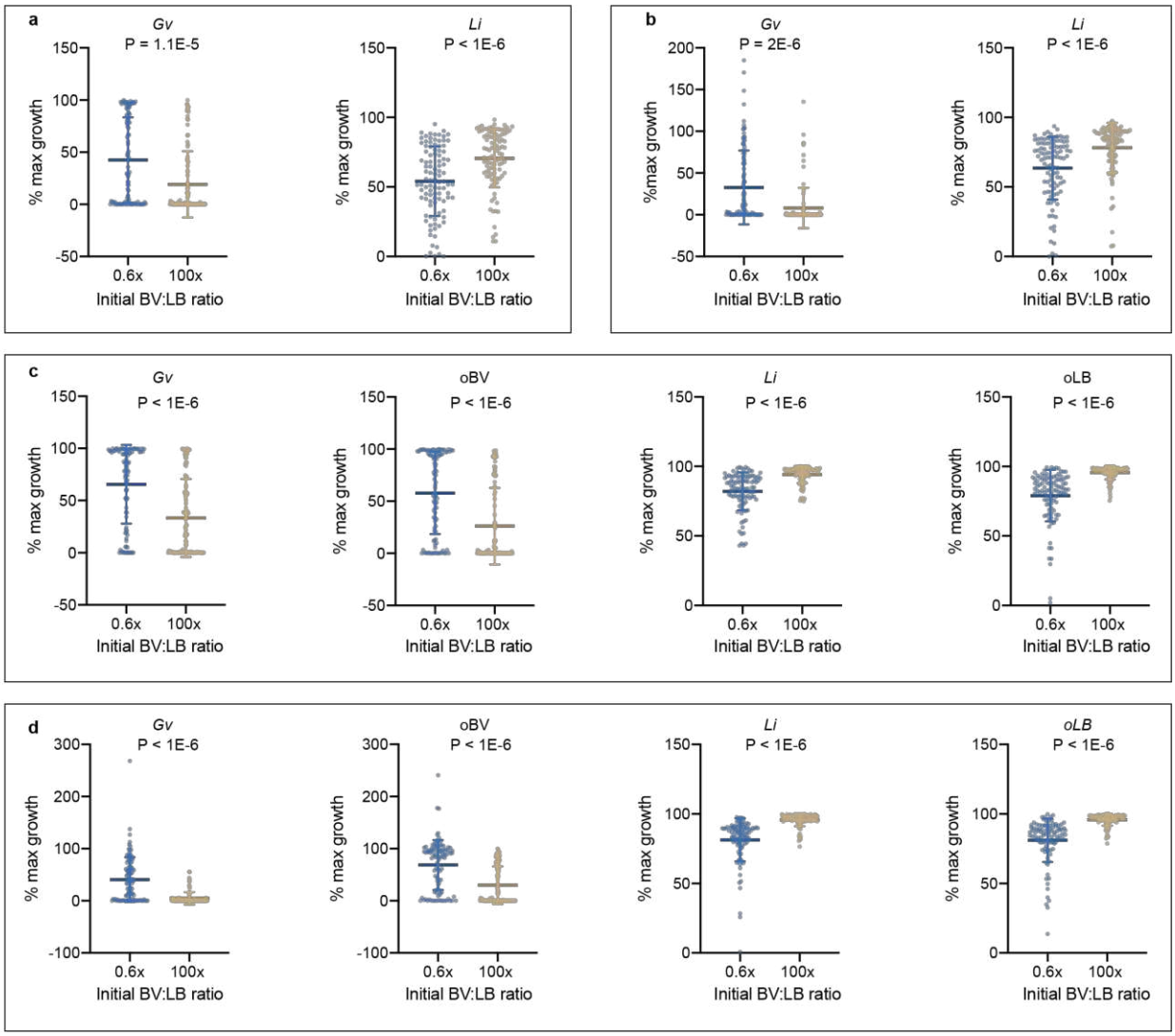

Supplementary Figure 6: BV:LB ratios influence endpoint BV-associated bacteria and *Lactobacillus* spp. abundances even with strain variation. (a) Model A: two species, no interactions proportion of maximal growth for *Gv* and *Li.* (b) Model B: two species with interactions proportion of maximal growth for *Gv* and *Li.* (c) Model C: four species, no interactions proportion of maximal growth for *Gv,* other BV-associated bacteria (oBV), *Li*, and other *Lactobacillus* sp. (oLB) (i – l) Model D: four species, with interactions proportion of maximal growth for *Gv,* other BV-associated bacteria (oBV), *Li*, and other *Lactobacillus* sp. (oLB). Lines indicate mean and standard deviation,

multiple unpaired two-tailed t-test p-values were adjusted using Benjamini and Hochberg correction.

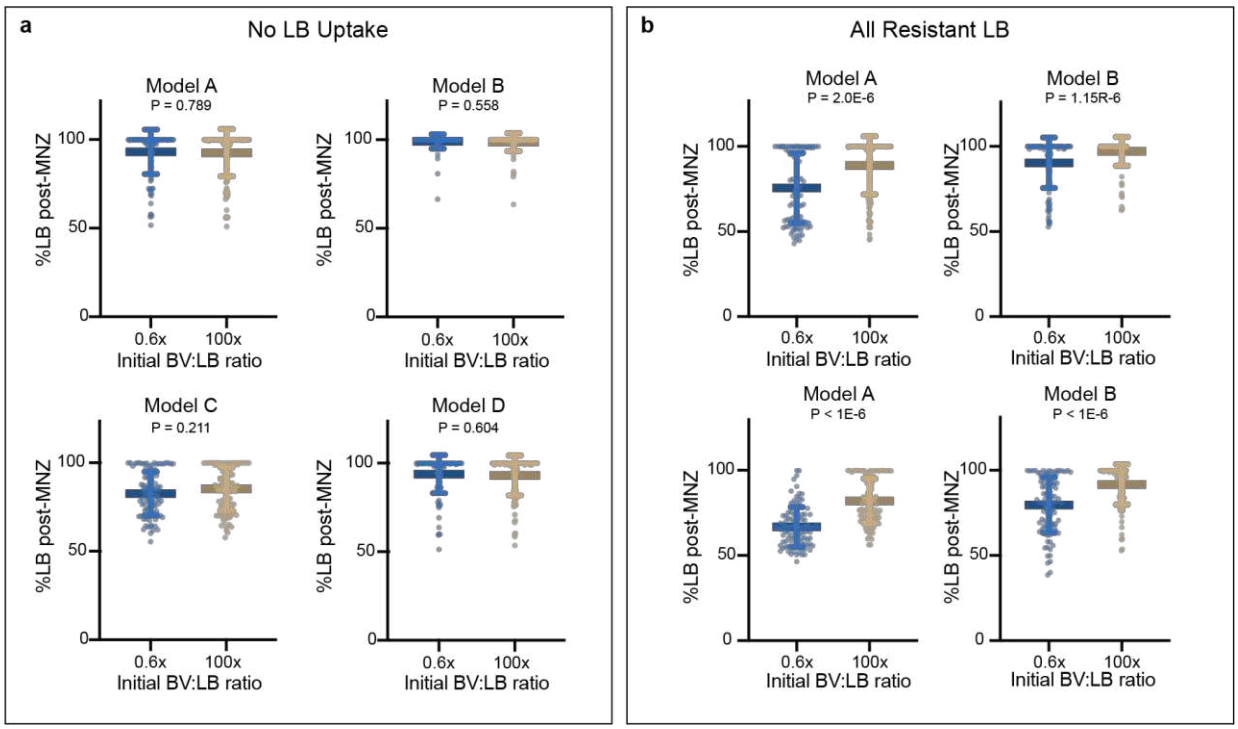

Supplementary Figure 7: Uptake or Sequestration of *Lactobacillus* spp. with MNZ drives initial BV:LB ratio influence of MNZ efficacy. (a) Post-treatment proportion of *Lactobacillus* sp. for Models A – D at 48h with 500 μg/ml MNZ with the rate of internalization of all *Lactobacillus* spp. (LB) set to zero (b) Post-treatment proportion of *Lactobacillus* sp. for Models A – D at 48h with 500 μg/ml MNZ with the EC50 set to 10,000 μg/ml for all *Lactobacillus* spp. (LB). Lines indicate mean and standard deviation, multiple unpaired two-tailed t-test p-values were adjusted using Benjamini and Hochberg correction.

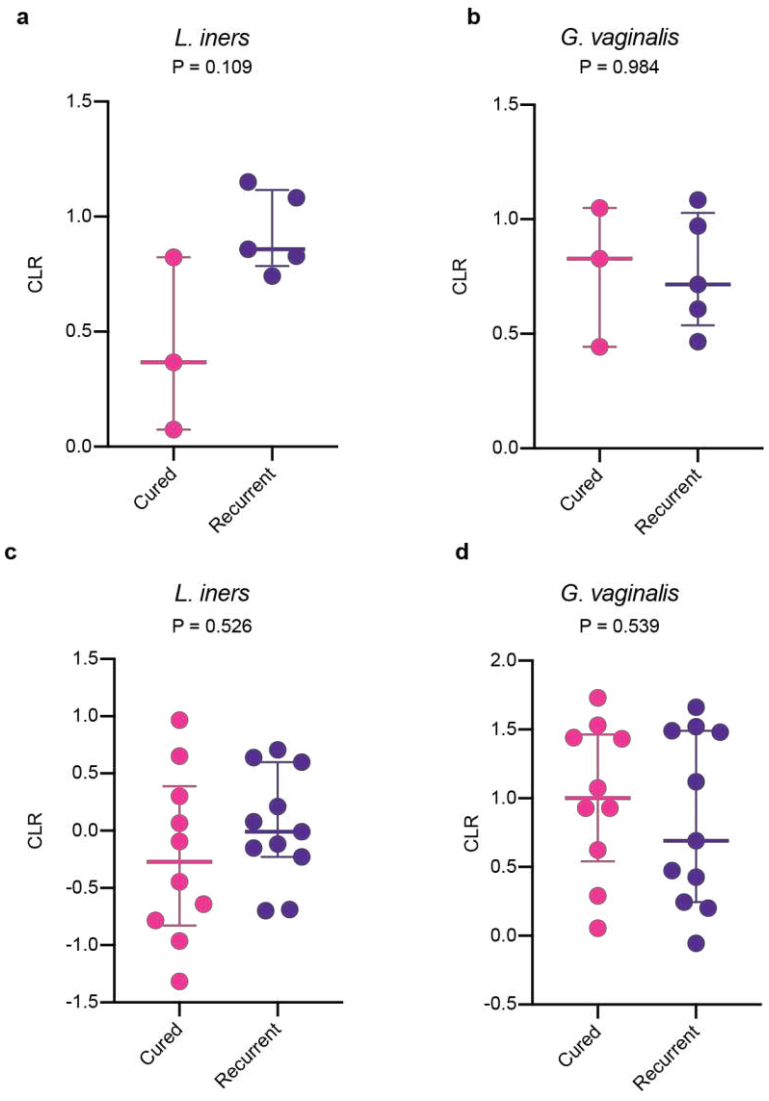

Supplementary Figure 8: Initial relative abundance data for *L. iners* and *G. vaginalis* for clinical outcomes. (a-b) UMB-HMP cohort for CLR-transformed relative abundances of (a) *L. iners* and (b) *G. vaginalis* (c-d) CONRAD BV cohort CLR-transformed relative abundances for (c) *L. iners* and (d) *G. vaginalis*. One-way unpaired t-test, central mark indicates median, bottom and top edges of the box represent the 25th and 75th percentiles and whiskers extend to most extreme data points that are not outliers.

678

Table S1: Model parameters.

Parameter Name	Description	Value	Units	Ref
$k_{int\text{-}GV}$	internalization rate of MNZ into GV	0.0139	cell density^{-1}hr^{-1}	[1]
$k_{grow\text{-}GV}$	maximal growth rate of GV	0.2269	hr^{-1}	[2]
K_{GV}	carrying a capacity for GV	4.2	cell density (10^6/mL)	[2]
$k_{kill\text{-}GV}$	kill rate of MNZ on GV	1.004	hr^{-1}	[3]
$EC50_{GV}$	concentration of MNZ to kill 50% of GV	420	µg/mL	[3]
k_{met}	rate of MNZ conversion to unknown metabolites	0.0174	cell density^{-1}hr^{-1}	[1]
$k_{int\text{-}LI}$	internalization rate of MNZ into LI	0.0042	cell density^{-1}hr^{-1}	[1]
$k_{grow\text{-}LI}$	maximal growth rate of LI	0.2309	hr^{-1}	[2]
K_{LI}	carrying a capacity for LI	3.569	cell density (10^6/mL)	[2]
$k_{kill\text{-}LI}$	kill rate of MNZ on LI	1.049	hr^{-1}	[3]
$EC50_{LI}$	concentration of MNZ to kill 50% of LI	598.87	µg/mL	[3]

[1] Determined from fig. S1

[2] Determined from fig. S2a & b

[3] Determined from fig. S2c & d

Table S2: Intraspecies Parameter Ranges

	Units	*G. vaginalis*	Other BV-associated	*L. iners*	Other *Lactobacillus*
1) k_{int}	cell density^{-1}hr^{-1}	0.015 – 0.15	0.0 – 0.20	0.0015 – 0.15	0.0 – 0.10
2) k_{grow}	hr^{-1}	0.20 – 0.60	0.20 – 0.40	0.20 – 0.80	0.20 – 1.00
3) K	cell density (10^6/mL)	3.0 – 4.5	2.0 – 4.5	3.0 – 5.0	3.0 – 5.0
4) EC50	µg/mL	50 - 500	50 - 500	400 – 4,000	400 – 4,000
5) k_{kill}	hr^{-1}	1	1	1	1
6) k_{met}	cell density^{-1}hr^{-1}	0.005 – 0.05	0.005 – 0.05	0	0

Table S3: Inter-species interaction terms. These terms descript the fold change in bacterial population that occurred from monoculture compared co-culture, a number greater than 1 indicates an increase in growth and less than 1 indicates an inhibition of growth.

		Source ($f_{s->t}$)			
		Gv	**oBV**	**Li**	**oLB**
Target	**Gv**		1.0 – 1.3	1.0 – 1.0	1x10^{-6} – 1.0
	oBV	1.0 – 2.5		1.0 – 1.0	1x10^{-6} – 1.0
	Li	1.0 – 1.0	1.0 – 1.0		1.0 – 1.3
	oLB	1.0 – 1.0	1.0 – 1.0	1.0 – 1.3	

Table S4: Relative abundances of prevalent bacteria in BV for the UMB-HMP cohort.

Patient ID	*L. iners*	*G. vaginalis*	*L. crispatus*	*A. vaginae*	*L. jensenii*	*other anaerobes*
UAB128	0.492	0.337	0.008	0.032	0.007	0.124
UAB003	0.372	0.336	0.077	0.028	0.014	0.173
UAB005	0.318	0.272	0.039	0.141	0.021	0.210
UAB035	0.348	0.238	0.131	0.068	0.007	0.209
UAB053	0.520	0.189	0.065	0.050	0.027	0.149
UAB127	0.093	0.448	0.015	0.172	0.002	0.270
UAB130	0.047	0.273	0.001	0.263	0.000	0.416
UAB135	0.394	0.164	0.033	0.074	0.002	0.333

Grey shading denotes patients that exhibited recurrent BV.

Table S5: Relative abundances of prevalent bacteria in BV for the CONRAD BV cohort.

Patient ID	Gv:Li Ratio	*G. vaginalis*	*L. iners*
24_v1	4.606	0.348	0.075
25_v1	1.793	0.030	0.017
26_v1	0.051	0.008	0.161
27_v1	4.257	0.017	0.004
28_v1	1.519	0.063	0.042
29_v1	3.882	0.021	0.006
30_v1	0.722	0.015	0.020
31_v1	3.096	0.125	0.040
33_v1	7.276	0.145	0.020
34_v1	0.408	0.054	0.133
35_v1	2.726	0.345	0.126
14_v1	5.592	0.121	0.022
15_v1	4.602	0.032	0.007
16_v1	18.962	0.067	0.004
17_v1	14.635	0.124	0.009
18_v1	1.916	0.182	0.095
19_v1	0.933	0.016	0.018
20_v1	1.000	0.015	0.015
21_v1	16.337	0.034	0.002
22_v1	1.723	0.224	0.130
23_v1	10.784	0.013	0.001

Grey shading denotes patients that exhibited recurrent BV.

Base Model Equations

(1) $\frac{d[Li]}{dt} = [G_{Li} - D_{Li}] * [Li]$

(2) $\frac{d[Gv]}{dt} = [G_{Gv} - D_{Gv}] * [Gv]$

(3) $\frac{d[MNZ_{ext}]}{dt} = -k_{int\_LI} * [MNZ_{ext}] * [Li] - k_{int\_GV} * [MNZ_{ext}] * [Gv]$

(4) $\frac{d[MNZ_{int\_LI}]}{dt} = k_{int\_LI} * [MNZ_{ext}] * [Li] - D_{Li} * [Li] * \left[MNZ_{\frac{int}{Li}}\right]$

(5) $\frac{d[MNZ_{int\_GV}]}{dt} = k_{int\_GV} * [MNZ_{ext}] * [Gv] - k_{met} * \left[MNZ_{int_{GV}}\right] * [Gv] - D_{Gv} * [Gv] * [MNZ_{\frac{int}{Gv}}]$

(6) $\frac{d[Met]}{dt} = k_{met} * \left[MNZ_{int_{GV}}\right] * [Gv]$

$$D = k_{kill}\left(\frac{[MNZ_{int}]}{EC50 + [MNZ_{int}]}\right) \qquad G = k_{grow} * \left(1 - \frac{[cell\ density]}{K}\right)$$

$$MNZ_{int/cell} = \frac{[MNZ_{int}]}{[cell\ density] * V_{culture}} * V_{cell}$$

Equation (1) represents the growth dynamics of the *Li* population, (2) the *Gv* population, (3) the extracellular MNZ concentration (4) the bulk intracellular MNZ concentration for *Li* (5) the bulk intracellular MNZ concentration for *Gv* (6) the concentration of metabolites produced by *Gv*. "D" represents the death rate of the population and is dependent on the respective intracellular MNZ concentrations, EC50s and maximum kill rates. "G" represents the logistic growth of the respective populations dependent on the maximum growth rate and carrying capacities. "$MNZ_{int/cell}$" represents the mass of MNZ internalized in each cell and is dependent on the bulk concentration of MNZ, per cell (cell density * culture volume) and cell volume.

Figures

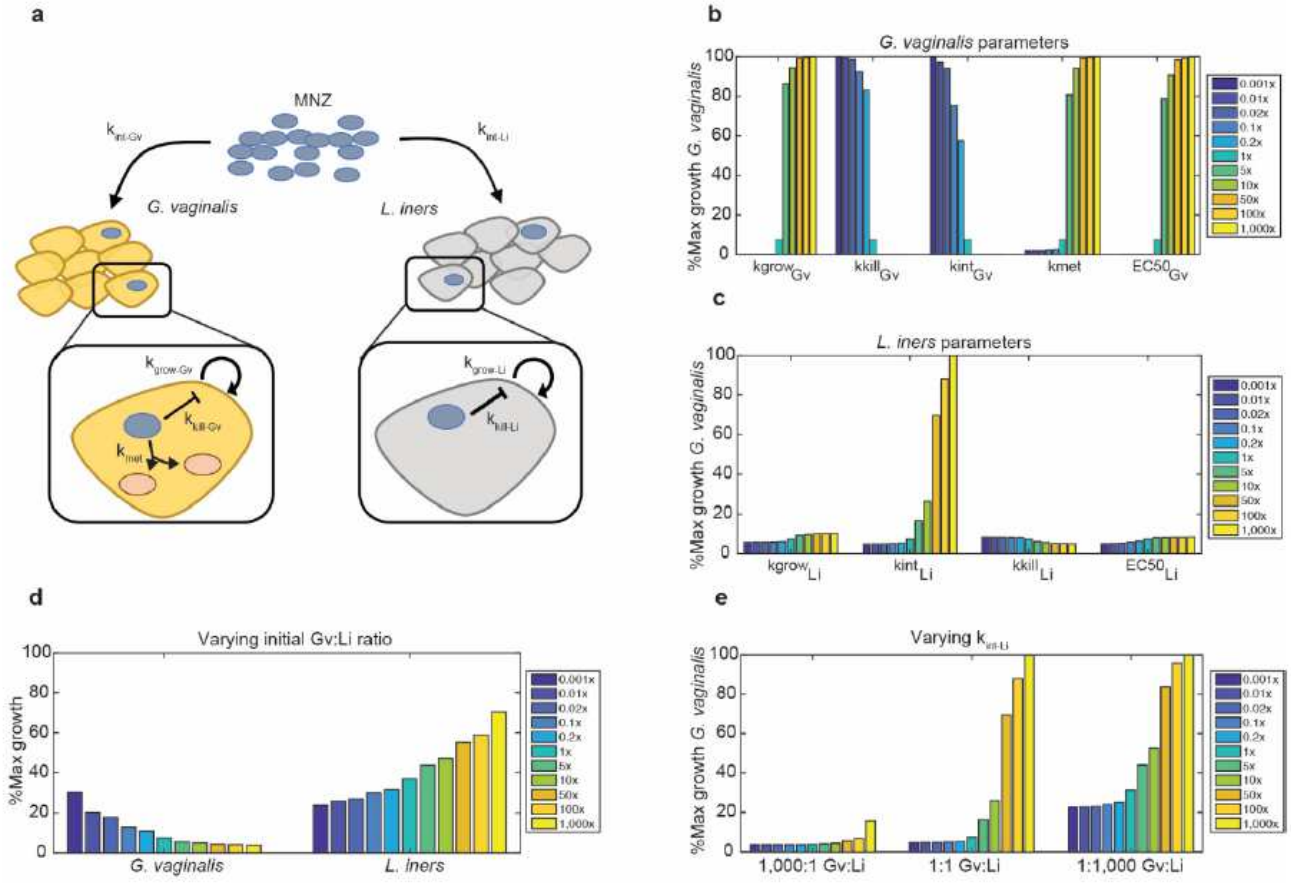

Figure 1

Model schematic for bacterial growth dynamics in BV with MNZ treatment. (a) MNZ is internalized by both G. vaginalis (Gv) and L. iners (Li) at rates kint-GV and kint-LI, cells are proliferating at kgrow-GV and kgrow-LI and MNZ inhibits growth by kkill-GV and kkill-LI. For G. vaginalis, a potential mechanism of MNZ resistance is the bacterial-mediated interactions to the drug leading to the formation of metabolites (kmet). (b) Sensitivity of Gv growth with 500 µg/ml MNZ when parameters directly related to Gv growth are varied 0.001x to 1,000x baseline values. Percent maximal growth refers to the final cell count compared to the carrying capacity of the culture, or the maximum cell count the unperturbed culture can reach at 48h based on initial cell counts (c) Sensitivity of Gv growth with 500 µg/ml MNZ when parameters related to Li survival are varied 0.001x to 1,000x baseline values. (d) Max growth of Gv (left) and Li (right) when the initial ratio of Gv to Li is varied with 500 µg/ml MNZ treatment. (e) Max growth of Gv when MNZ internalization rate of Li is varied at three different population compositions with 500 µg/ml MNZ treatment.

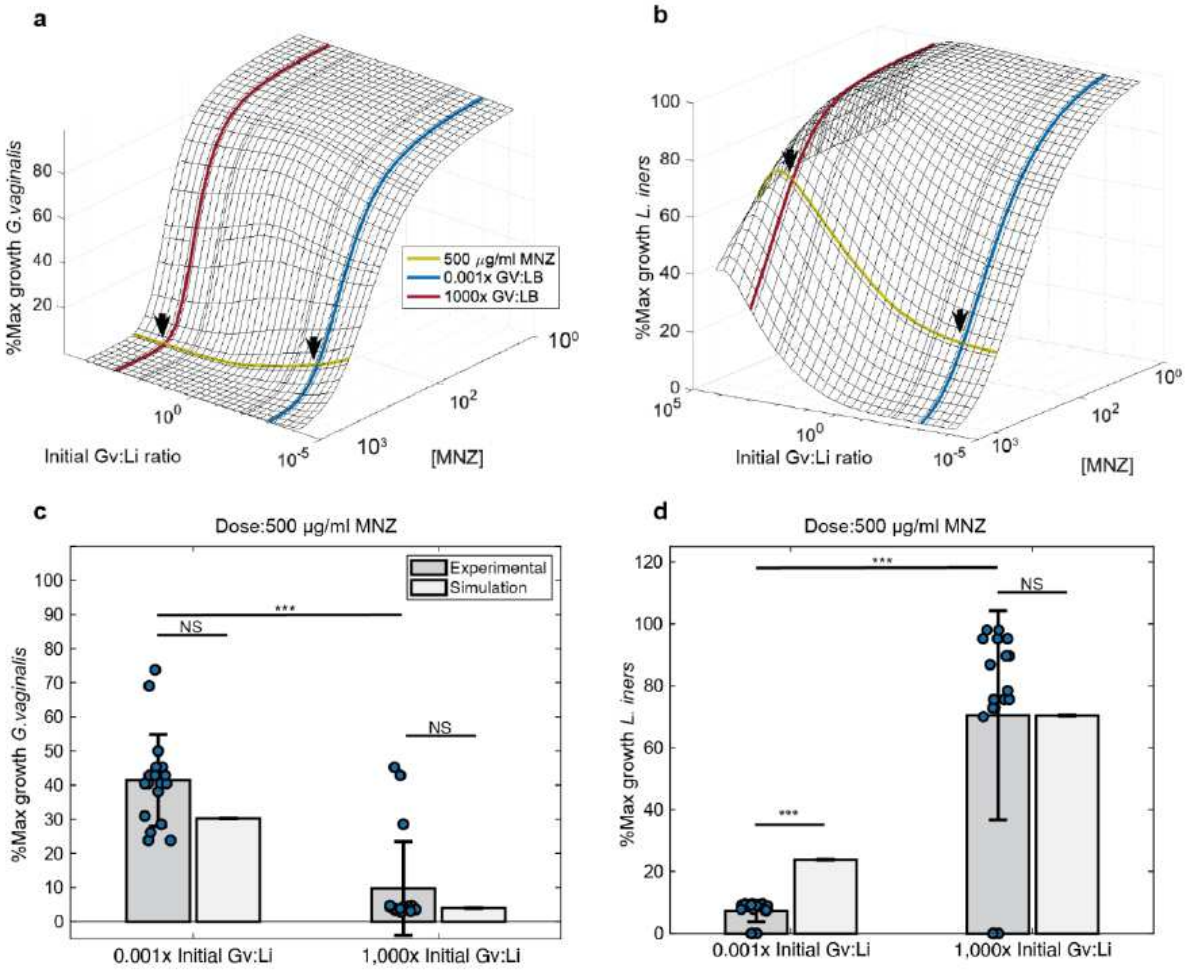

Figure 2

A higher initial Gv:Li ratio improves MNZ treatment efficacy. (a) Surface plot to illustrate predicted percent maximal growth of Gv (z-axis) when concentration of MNZ (x-axis) and the ratio of Gv:Li (y-axis) are varied in simultaneously. Arrows indicate the concentration of MNZ and ratios of Gv:Li used for model validation. (b) Percent maximal growth of Li after simultaneous variation of MNZ dose and Gv:Li ratio. (c-d) Comparison of model simulations to experimental data for 500 μg/ml MNZ at 1000x and 0.001x Gv:Li (* $p < 0.05$, ** $p < 0.01$, *** $p < 0.001$, unpaired two-tailed t-test, error bars represent standard deviation).

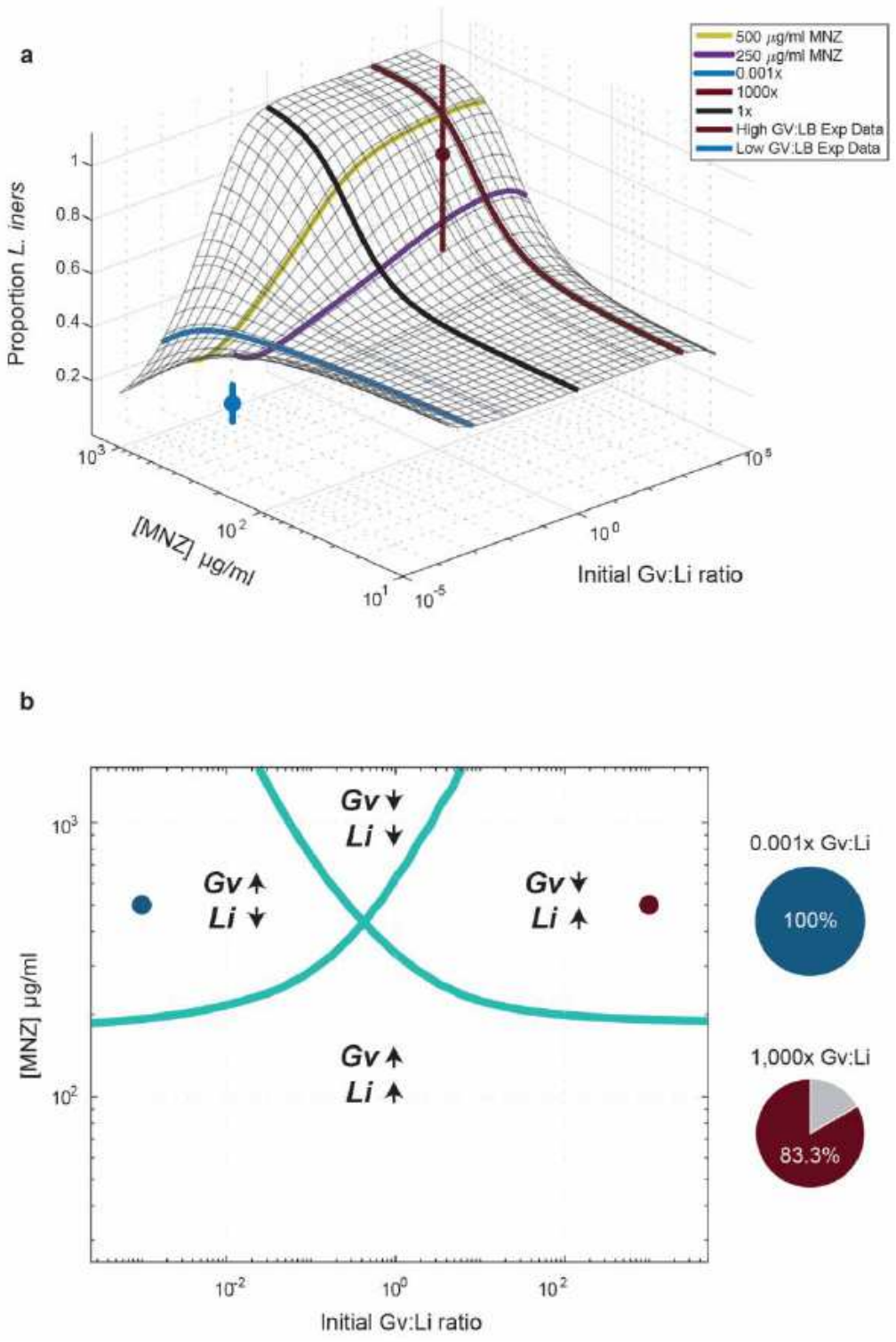

Figure 3

Initial Gv:Li ratios dictate final microbial populations. (a) Surface plot illustrates model predictions for proportion of Li relative to Gv 48h at different starting Gv:Li ratios (x-axis) and at different doses of MNZ (y-axis). Experimental validation was performed in in vitro co-cultures of Li and Gv (n = 36) and is plotted on the surface, with mean and ± standard deviation represented by nodes and vertical lines (b) Phase diagram of microbial growth dynamics 48hrs after exposure to various MNZ doses, dots indicate

experimental conditions evaluated. There are four possibilities: Both Gv and Li populations are increased after treatment, both Gv and Li populations are decreased, only the Gv population is increased and only the Li population is increased. Pie charts indicate the fraction of experimental samples that agree with the predicted trends (right).

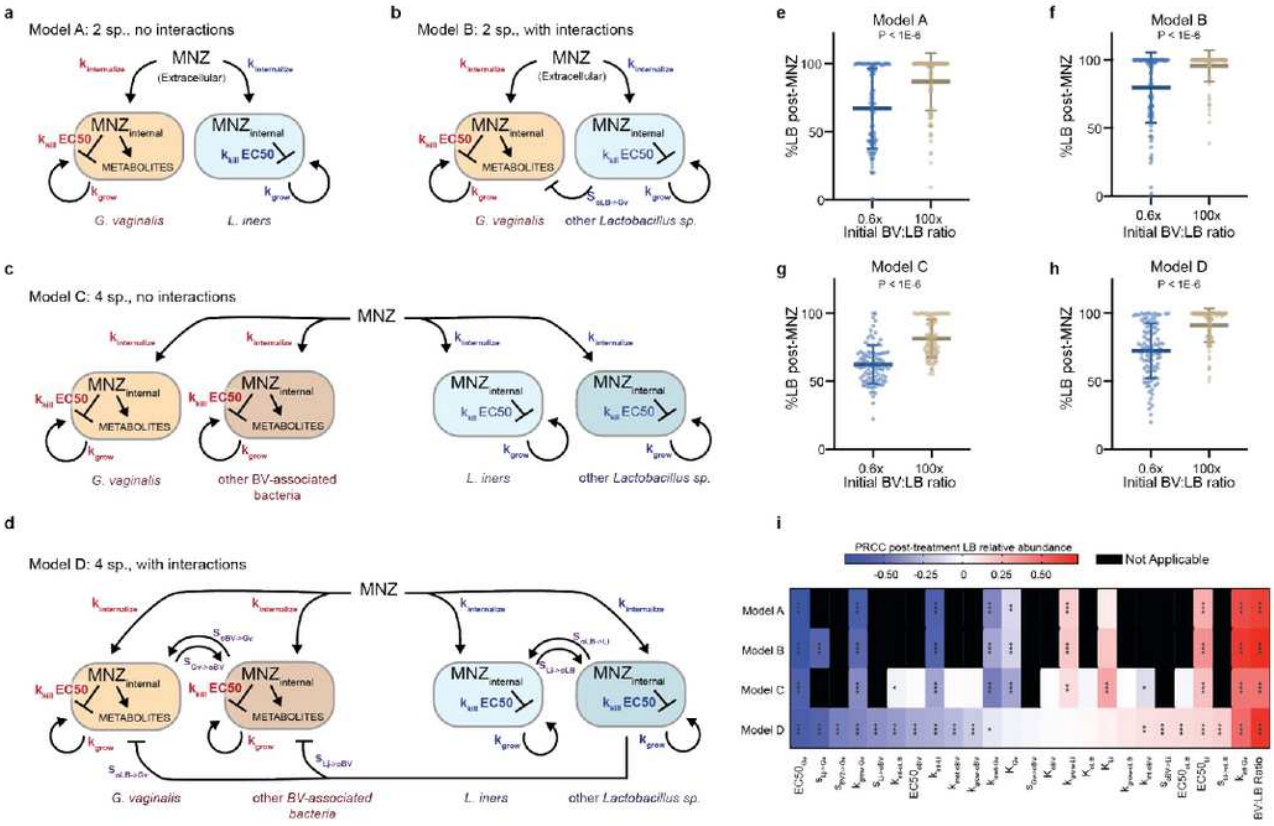

Figure 4

High pre-treatment BV:LB ratio is predicted to reduce MNZ efficacy in more complex microbial environments regardless of strain variability. (A) Original model structure validated in Fig. 2 (B) Two species model with negative interaction between other Lactobacillus sp. (oLB) and Gv (c) Four species model of Gv and Li with additional representative bacteria for BV-associated bacteria and Lactobacillus sp. (d) Four species model with inter-species interactions. Within BV-associated bacteria and Lactobacillus sp. interactions were simulated from mutualistic (both benefit) to commensal (one benefits, the other is neutral). Inhibitory (amensal) interactions are included between D-lactic acid producing bacteria, other Lactobacillus sp., with both BV-associated bacteria (e-h) post-MNZ treatment (48h, 500 µg/ml) Lactobacillus sp. relative abundances at. 0.6x and 100x BV-associated bacteria to Lactobacillus sp (BV:LB) ratios. Each point represents a parameter set randomly sampled from physiological ranges in Tables S2 and S3 (i) Significantly sensitive parameters (assessed by partial rank correlation) for each model structure (a-d) as determined by the global sensitivity and uncertainty analysis.

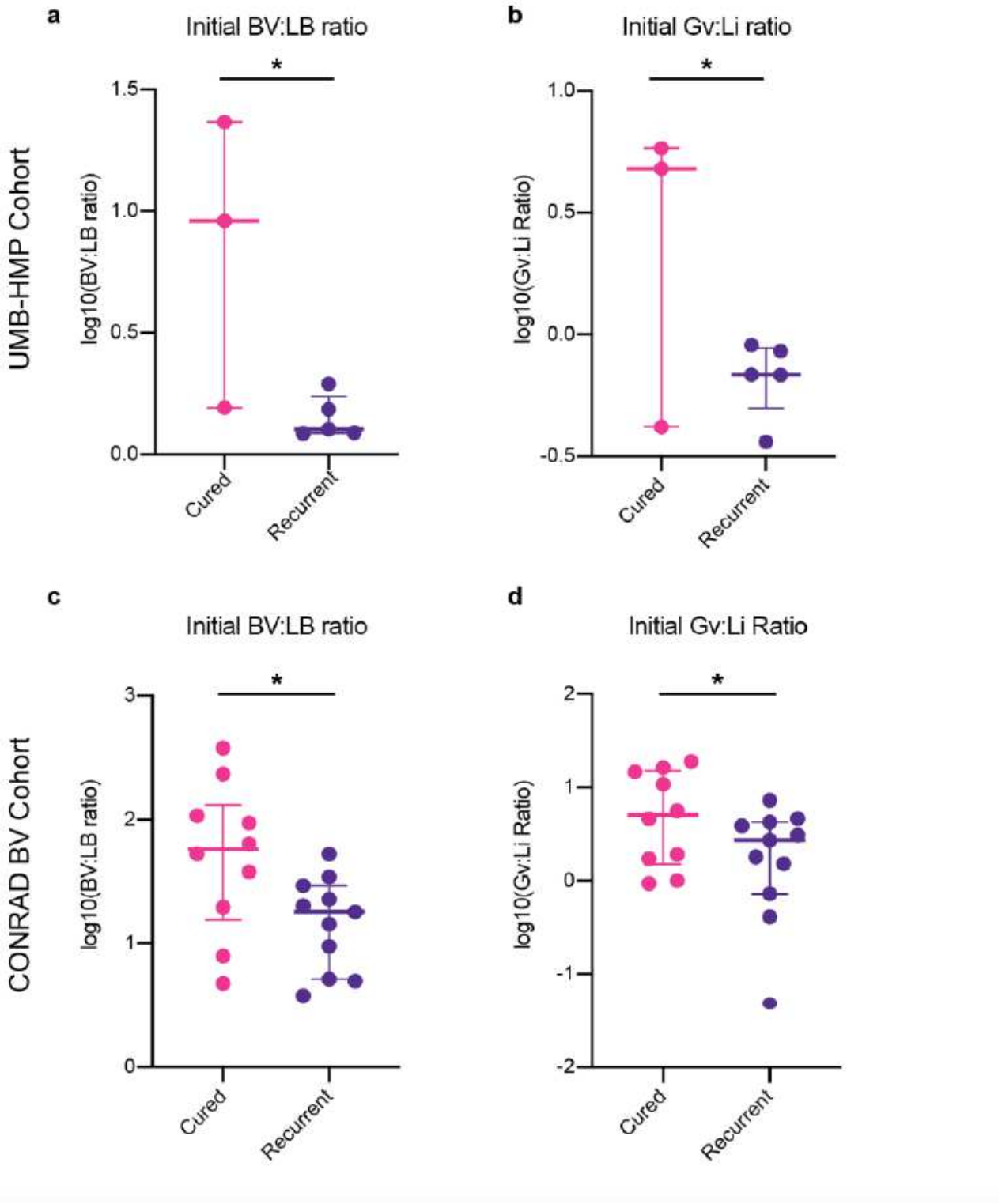

Figure 5

Increased initial BV:LB ratios associated with successful treatment of BV. (a – b) clinical results for the UMB-HMP cohort describing the (a) log base 10 transform of initial BV-associated bacteria relative abundance to Lactobacillus sp. relative abundance (b) initial Gv:Li ratio. (c – d) Clinical results for the CONRAD BV cohort (c) log base 10 transform of initial BV-associated bacteria relative abundance to Lactobacillus sp. relative abundance. (d) initial Gv:Li ratio. Lines depict the 25th, 50th and 75th

percentiles, multiple unpaired one-tailed t-test p-values were adjusted using Benjamini and Hochberg correction.